

Analysis of PD and Nonlinear Control of Mechanical Systems with Dynamic Backlash

M. T. MATA-JIMÉNEZ

Faculty of Electrical and Mechanical Engineering, University of Nuevo León, C.U. Pedro de Alba S/N, San Nicolás de los Garza, Nuevo León, Mexico

B. BROGLIATO

INRIA Rhône-Alpes, ZIRST Montbonnot, 655 Avenue de l'Europe, 38334 St. Ismier, Cedex, France

(Received 8 April 2001; accepted 6 August 2001)

Abstract: In this paper, we focus on the analysis and control of a simple rigid-body mechanical system with clearance. Contrary to most of the existing works in the literature concerning control, we explicitly treat all the nonlinear non-smooth characteristics of this system considered as a rigid-body mechanical system with unilateral constraints and impacts (dynamic backlash). The model is therefore a hybrid dynamical system, mixing discrete events as well as continuous states. The regulation and tracking capabilities of the proportional-derivative (PD) scheme are investigated. In particular, a complete proof of the existence of a limit cycle for non-collocated PD control is provided, including viability constraints. It is concluded that tracking requires the development of specific control schemes. Consequently, we propose a hybrid control that may be used to track some desired trajectories in conjunction with a PD input. Throughout the paper, the particular features of unilaterally constrained mechanical systems are taken into account, such as the fundamental viability property of closed-loop solutions and controls. This work is a new approach to be considered for application in several areas including the control of kinematic chains with joint clearance and vibro-impact systems, as well as liquid slosh control. Numerical results are presented to illustrate the possible performance of the proposed control scheme and its robustness properties.

Key Words: Mechanical systems, dynamic backlash, impacts, non-smooth hybrid dynamics

1. INTRODUCTION

Backlash nonlinearities cause delays, oscillations, and consequently give rise to inaccuracies in the position and velocity of the machine (Dagalakis and Myers, 1985; Podsedkowski, 1997). Backlash commonly occurs in bearings, gears and impact dampers, and methods to automatically measure clearance evolution in kinematic chains are being developed (Podsedkowski, 1992). It arises from unavoidable manufacturing tolerances or is often deliberately incorporated in the system to accommodate thermal expansion (Bapat et al., 1983). In previous investigations, Tao and Kokotovic (1995) analyzed the problem and proposed to model backlash as a hysteresis function between the output and input positions of

the system. This is a kinematic model since the dynamic effects of the collisions are not taken into account. Such a model is based on the assumption that the shocks are purely inelastic and that the ratio of the inertias of the two interacting masses is zero. This is met in some practical applications to which such control schemes may be applied successfully.

Using a similar model, Tang et al. (1997) have proposed a simple switching control strategy, which consists of accelerating the motion in the backlash phase. The impact effects have not been analyzed and no details are given on the properties of the material which collide. Experimental results on a CNC machining center performing a circular motion (radius 150 mm) are provided. The linear table speed is 8.33×10^{-3} m/s, which is a low impacting relative velocity. The backlash size is found after identification to be around 0.5 mm, and the tracking error is about the same size. They have shown that the backlash compensation significantly improves the tracking properties compared to a linear controller. The introduction of a dither into systems with backlash has been extensively studied for years; see Hsiao and Hwang (1997) and references therein. For this approach, the kinematic model is used. The goal of this technique is to eliminate the memory of the static nonlinearity by injecting a high-frequency signal. In this method an approximated smoothed system is obtained. Azenha and Tenreiro Machado (1996) have investigated the control of a system with dynamic backlash, i.e. the impacts and inertial effects are incorporated in the model. In order to explore the limit cycle behavior of the system, they have based their analysis on the describing function techniques. Their study is carried out by means of numerical simulations. The dynamic equations of motion for an impact pair including compliance at the contact have been formulated by Nordin (1993) and Nordin et al. (1997). It is assumed that the system is an inertia-free elastic shaft system with backlash. The proposed linear control input uses a low gain when the system evolves inside the clearance. They have justified the choice of the compliant contact/impact model by citing laboratory experimental results. In a recent paper, Indri and Tornambè (1997) have dealt with mechanical gears with backlash and elasticity in the joints. In order to control the system, they have proposed a collocated proportional-derivative (PD) controller for regulation. The properties of the closed-loop solutions are obtained and the stability of this strategy is proven. A system with purely inelastic impacts has been studied in Chalhoub and Zhang (1996). The regulation control technique consists in accelerating the controlled gear to shorten the disengagement period when the second gear is uncontrolled. There is no stability proof. Experimental validation on a flexible beam controlled by an axis with gear play is presented. The instant of disengagement of the gears is detected in order to switch the control. Yeh et al. (1996) have proposed a compliant model to describe the backlash phenomenon and, exploiting this model, a nonlinear adaptive control has been designed. They have demonstrated the semi-global stability of the scheme for tracking purposes. A system that is used in industrial applications has been described in Fanuc (1994). It consists of a tandem control (two actuators) for positioning manufacturing pieces and controlling machine-tool tables. This industrial application shows that somewhat sophisticated controllers, with switching conditions and detection of the backlash phases, can be implemented. Several other backlash models have been proposed and studied in the mechanical engineering literature (Stepanenko and Sankar, 1986) and, in particular, in relation to the so-called impact damper. Bapat et al. (1983), Li et al. (1990) and Shaw and Rand (1989) have studied the dynamic response of simplified rigid-body impacting systems. They have shown the existence of complex dynamics including different types of periodic trajectories, bifurcations, and chaotic motion. In Pfeiffer and Glocker (1996)

a detailed analysis of the rigid-body model has been proposed, together with experimental results that corroborate the theoretical investigations (Reithmeier, 1991; Pfeiffer and Kunert, 1990; Kunert and Pfeiffer, 1991).

In this work, the impact damper (see Figure 1) is used as a simplified model of backlash for feedback control purposes incorporating the dynamical effects of impacts. We use a rigid-body model which is justified by typical numerical values of 10^{10} N/m for the contact/impact stiffness and a contact damping of 10 Ns/m between metals that have been reported in the literature (Deck and Dubowsky, 1994; Smith, 1983). For instance, consider a simple system that consists of a mass striking a rigid wall. If the contact/impact process is modeled by a spring with stiffness $k = 10^7$ N/m, simple calculations (Brogliato, 1999) yield an impact duration of 10^{-3} s for $m = 1$ kg. Then the impact can be considered instantaneous. In our opinion, the rigid-body approach, which incorporates dynamical effects of impacts and unilaterality of the constraints, may be quite a useful model for control design for several reasons. Firstly, it is a model which is simple enough (therefore allows us to derive and study controllers), yet which incorporates some highly nonlinear effects, namely impacts and unilaterality. Secondly, such models have been validated experimentally elsewhere for much more complex systems (Abadie, 2000; Pfeiffer and Glocker, 1996). In particular, it is clear that high values of the contact stiffness preclude the use of control inputs which directly incorporate k , since this would yield high gains in the control loop and unacceptable control input magnitude. Such control schemes (see, for example, Tao et al. (2001)) are therefore limited to small contact stiffness values, which often lack practical realism.

The goal of this paper is first to study the limitations of PD controllers. The regulation problem is examined, extending in a logical way the work of Indri and Tornambè (1997) towards the rigid-body model for the collocated case. The existence and stability of limit cycles in the non-collocated case are also carefully studied and a completely analytical proof is given, which apparently has never been proposed in the literature for such a four-dimensional non-smooth mechanical system. Then we focus on the tracking problem. When considering a PD controller, the first problem we have to face when we want to track a path $x_d(t)$ is: are there a couple of gains (k_p, k_v) such that, under ideal conditions, the trajectory $x_1(t) = x_d(t)$ exists? Although the answer to this question when the clearance is zero is trivial if $x_d \in C^2[\mathbb{R}^+]$, it becomes more cumbersome when the clearance is strictly positive. In the present work, we choose to examine particular trajectories (periodic, one impact per period, symmetric) for which existence results can be proven. A major conclusion is that the set of trajectories that we can identify analytically, so that a PD controller can be used for tracking purposes, is rather small, and lacks practical usefulness in general. It is however not *a priori* excluded that other types of orbits may exist and may be tracked with a PD input, but the analytical proof of their existence is an open problem. Now, another point of view is that of considering a desired orbit and finding a tracking controller (not necessarily linear). To this aim, we propose a hybrid control strategy. The first motivation is to provide a complementary control that can be considered as a *safety net* around the (possibly small) region of attraction of the linear controller orbit (Guckenheimer, 1995). In contrast to other types of existing hybrid control strategies for the full system based on the use of chaotic motion to bring the system into the basin of the desired motion (Ott et al., 1990), the proposed strategy guarantees transient properties. Two controllers are proposed: a constant and impulsive controller and another piecewise constant controller. Most importantly, these controllers are also shown to have a possible application in the (approximate) tracking control problem of certain time

varying trajectories, in conjunction with a PD input, hence improving the (generally poor) tracking capabilities of PD controllers. Throughout the paper, we pay particular attention to the so-called viability conditions (a definition is given later), which play an essential role in the analysis and control of systems with unilateral constraints (Babitsky, 1998). The main difference between the proposed hybrid controller (here called PD+) and some of the aforementioned controllers is that it does not aim at minimizing the velocity during the backlash phases (to decrease collision effects), nor at establishing a direct transfer from one constraint to the other. Rather, it uses impacts to drive the system between two points of its state space through a sequence of suitable collisions.

2. CONTROLLED IMPACT DAMPER MODEL

The consideration of an impact damper, composed of a free object constrained to move in a slot inside a controlled mechanism, allows us to clearly highlight the features due to unilateral constraints and collisions while keeping the rest of the dynamics quite simple. This is a system that can be considered as a particular case of nonlinear non-smooth hybrid systems with complementarity conditions (for frictionless constraints) given by (Brogliato, 1999; Lötstedt, 1982)

$$\begin{aligned} M(q)\ddot{q} + F(q, \dot{q}) &= E(q)U + \nabla h \cdot \lambda \\ h(q) &\geq 0, \quad \lambda^T h(q) = 0, \quad \lambda \geq 0 \end{aligned} \quad (1)$$

Collision rule

where U is the control input, λ is the vector of Lagrange multipliers, $h(q)$ is the unilateral constraint vector and a restitution law is needed to complete the model. Notice that equation (1) can represent several different control systems including juggling systems (see Brogliato and Zavala Río (2000) and Zavala Río and Brogliato (1999)) and manipulators performing complete robotic tasks (Brogliato, 1999; Brogliato et al., 2000). However, the analysis and control of such complementarity systems still need to be investigated.

A schematic diagram of the mechanical system under consideration is shown in Figure 1. It consists of a primary mass m_1 that is constrained to move in a slot inside a secondary mass m_2 , which is subject to an external control input U . The supposed frictionless motion of m_1 is instigated by collisions with m_2 , which occur intermittently because of the clearance $2L$. This idealized model is called an *impact pair*. Because of its simplicity, it has been used frequently as a basic model for the study of mechanical systems with clearance; see Bapat et al. (1983), Brogliato (1999), Shaw and Rand (1989) and Stepanenko and Sankar (1986) and references therein. Although it is an approximate model, it exhibits the typical behavior found in such systems and has an extremely rich dynamics. It is also used in aeronautics to control or damp vibrations of structures (such as helicopter blades and rotors), as well as to model the dynamics of fuel tanks (known as the liquid slosh phenomenon) (Hung and Pan, 1996; Ibrahim and Sayad, 1998; Pilipchuk and Ibrahim, 1997).

The motion of the system can be decomposed in three phases: *the backlash phase* Ω , during which the primary mass flies freely between the constraints without reaching them; *the impact phase* I , when the contact of the masses is established with non-zero relative velocity, i.e. the primary mass impacts one constraint; the third phase, *the contact phase* C , is obtained

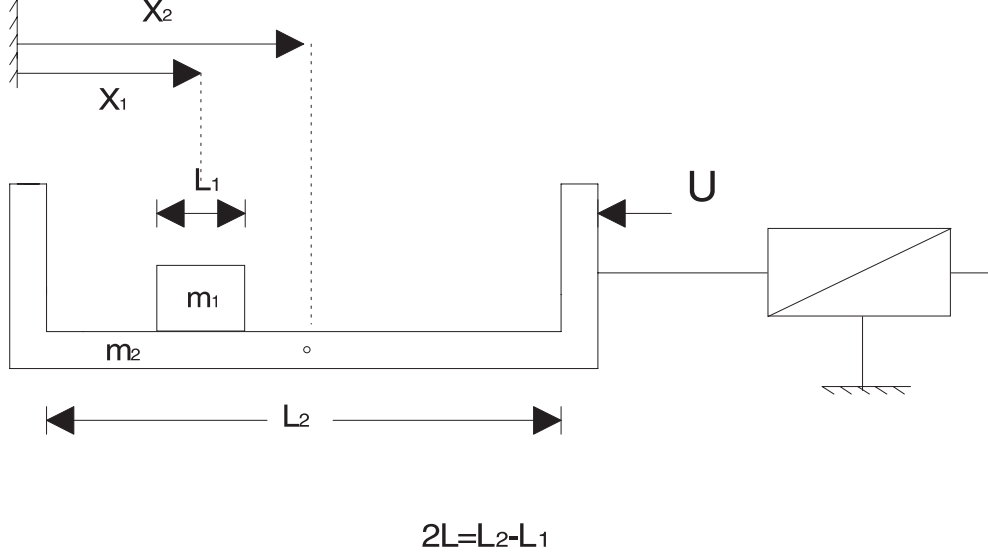


Figure 1. Physical model.

when the relative velocity of the system is zero at the contact instant or after the collision. In this phase, the two masses remain engaged. Using Newton's law for collisions, the equations governing the motion are given by (the analogy with equation (1) is clear)

$$\begin{aligned}
 m_1 \ddot{x}_1 &= \lambda_1 - \lambda_2 \\
 m_2 \ddot{x}_2 &= U - \lambda_1 + \lambda_2 \\
 h_1(x_1, x_2) &= L + x_1 - x_2 \geq 0 \\
 h_2(x_1, x_2) &= L - x_1 + x_2 \geq 0 \\
 \dot{x}_1(t_k^+) - \dot{x}_2(t_k^+) &= -e(\dot{x}_1(t_k^-) - \dot{x}_2(t_k^-))
 \end{aligned} \tag{2}$$

where x_1 and x_2 represent the displacements of the primary and secondary masses respectively, and e is a restitution coefficient (Brogliato, 1999).¹ The backlash phases dynamics is obtained by setting $\lambda_1 = \lambda_2 = 0$, whereas the contact phases dynamics corresponds to either ($\lambda_1 > 0$ and $\lambda_2 = 0$) or ($\lambda_1 = 0$ and $\lambda_2 > 0$). Notice that in the backlash phases the system is underactuated in the sense that there is only one control input and two degrees of freedom; the primary mass is unaffected by the action of the input. In the impact phase, the behavior of the system at the collision time t_k is given by (with the percussion $p_i > 0, i = 1, 2$)

$$\begin{aligned}
 m_1(\dot{x}_1(t_k^+) - \dot{x}_1(t_k^-)) &= p_1 \quad (\text{or } -p_2) \\
 m_2(\dot{x}_2(t_k^+) - \dot{x}_2(t_k^-)) &= -p_1 \quad (\text{or } p_2)
 \end{aligned} \tag{3}$$

where $f(t_k^+)$ and $f(t_k^-)$ denote the left and right limits of a function $f(\cdot)$ at the k th impact. From equations (2) and (3), and since the positions of the masses are not changed during the

impact (Brogliato, 1999), the following relations can be obtained

$$\begin{pmatrix} x_1(t_k^+) \\ x_2(t_k^+) \\ \dot{x}_1(t_k^+) \\ \dot{x}_2(t_k^+) \end{pmatrix} = \begin{pmatrix} 1 & 0 & 0 & 0 \\ 0 & 1 & 0 & 0 \\ 0 & 0 & \frac{\mu-e}{1+\mu} & \frac{1+e}{1+\mu} \\ 0 & 0 & \frac{(1+e)\mu}{1+\mu} & \frac{1-\mu e}{1+\mu} \end{pmatrix} \begin{pmatrix} x_1(t_k^-) \\ x_2(t_k^-) \\ \dot{x}_1(t_k^-) \\ \dot{x}_2(t_k^-) \end{pmatrix}$$

$$\mathbf{X}(t_k^+) = \mathcal{E}(\mu, e) \mathbf{X}(t_k^-) \quad (4)$$

where $\mu = m_1/m_2$ is the mass ratio, X is the system state and \mathcal{E} is a constant matrix depending on the physical parameters. The motion of the system during the contact phase can be divided into two cases depending on the contact constraint. Using the complementarity conditions, it is a simple matter to prove that a sufficient condition for detachment is given by $U \text{sgn}(x_1 - x_2) > 0$. From equations (2) and (4), we can obtain a global representation of the system including the collision effects. It is important to notice that the behavior of the system is very complex because the equations representing the global system are a set of differential and algebraic equations. If we select a linear control input U , the system will be linear between collisions but globally nonlinear, due to the complementarity conditions and impacts.

3. PD CONTROL

For the ideal case ($L = 0$), the second-order system describing the system may be controlled via a PD controller of the form

$$U = m_2 \ddot{x}_d - k_v \dot{\tilde{x}} - k_p \tilde{x}, \quad k_p > 0, \quad k_v > 0 \quad (5)$$

where $\tilde{x} = x - x_d$ and x_d is a desired trajectory. This control is applied only on m_2 . For the system with $L \neq 0$, the control problem becomes much more difficult since the dynamics are as in equation (2). For feedback purposes, x can be chosen to be x_2 or x_1 . The first case is the *collocated control* and the second case is called the *non-collocated control*. The closed-loop behavior of the controlled system can be obtained by inserting equation (5) into equation (2), where in equation (5) $(x, \dot{x}) = (x_1, \dot{x}_1)$ for the non-collocated case and $(x, \dot{x}) = (x_2, \dot{x}_2)$ for the collocated case. In the following, we study the regulation and tracking cases separately.

3.1. Collocated regulation: global stability

If we choose a collocated control, the equations describing the system during the various phases are given by

$$\begin{aligned} \Omega : & \begin{cases} m_1 \ddot{x}_1 = 0 \\ m_2 \ddot{x}_2 = -k_p \tilde{x}_2 - k_v \dot{x}_2 \end{cases} \\ C : M \ddot{x} & = -k_p \tilde{x} - k_v \dot{x} \\ I : X(t_k^+) & = \mathcal{E}(\mu, e) X(t_k^-) \end{aligned} \quad (6)$$

where $M \triangleq m_1 + m_2$. For this control, the invariant set for the closed-loop system is given by

$$E = \{(x_1, x_2, \dot{x}_1, \dot{x}_2) \mid |x_1 - x_2| \leq L, x_2 = x_{2d}, \dot{x}_1 = 0, \dot{x}_2 = 0\} \subset \mathbb{R}^4 \quad (7)$$

which can also be characterized from a generalized equation, relying on the representation of the dynamics in equation (6) with convex analysis tools; see Brogliato (2001) and references therein. The stability analysis is based on the choice of a suitable unique positive definite function V of the partial system state $(\tilde{x}_2, \dot{x}_1, \dot{x}_2)$, as in Indri and Tornambè (1997):

$$V(\tilde{x}_2, \dot{x}_1, \dot{x}_2) = \frac{k_p}{2} \tilde{x}_2^2 + \frac{1}{2} (m_1 \dot{x}_1^2 + m_2 \dot{x}_2^2). \quad (8)$$

To analyze the stability of the whole system, we first investigate the stability of each phase independently. It is a simple matter to show that along the backlash and contact phases orbits, we obtain

$$\dot{V}(t) = -k_v \dot{x}_2^2(t) \quad (9)$$

which is negative semi-definite. Considering that the positions remain unchanged at the impact, we can calculate the jump at the collision times

$$\sigma_V \{t_{i_k}\} = -\frac{m_1 m_2}{2(m_1 + m_2)} (1 - e^2) (\dot{x}_1(t_{i_k}^-) - \dot{x}_2(t_{i_k}^-))^2 \leq 0 \quad (10)$$

for all $e \in [0, 1]$ and where $\sigma_V \{t_{i_k}\} = V(t_{i_k}^+) - V(t_{i_k}^-)$. Because $[x_2 < +\infty \Rightarrow x_1 < +\infty]$ we can conclude that the system is globally stable in the sense that the state remains bounded for all $t \geq 0$ and for all bounded initial conditions. It is interesting to notice that the collocated closed-loop system has a simple interpretation in terms of passive systems; the two subsystems in equations (2) and (6) with respective states (x_1, \dot{x}_1) and (\tilde{x}_2, \dot{x}_2) are clearly dissipative during the backlash phases with input $(\lambda_1 - \lambda_2, -\lambda_1 + \lambda_2)$ and output (\dot{x}_1, \dot{x}_2) , and the total system is dissipative at the collision times. The first property is lost in the non-collocated case. In Mata-Jiménez (1998) and Mata-Jiménez and Brogliato (1999), an analysis to demonstrate the asymptotic stability of the invariant set E for the collocated system has been proposed. Notice that, although the Krasovskii–LaSalle invariance principle may apply directly to such autonomous hybrid non-smooth systems, it is not available as such in the literature. Consequently, we have to prove asymptotic stability with a specific analysis. However, our goal in this paper is not to present a detailed analysis of the PD controller but rather to survey its capabilities and to propose a specific hybrid controller, see Section 4. Moreover, the asymptotic stability result is logical since the closed-loop system is autonomous and satisfies the conditions for existence and uniqueness of trajectories (Schatzman, 1998) as well as continuous dependence on initial conditions which are at the core of the invariance lemma (Vidyasagar, 1993). The proof of asymptotic convergence of closed-loop trajectories to the set (E) is therefore not presented.

Remark 1. Assume that x_d is time-varying but such that $\ddot{x}_d = 0$. For this particular case, we modify V in equation (8) as $V(\tilde{x}_2, \dot{x}_1, \dot{x}_2) = \frac{k_p}{2} \tilde{x}_2^2 + \frac{1}{2} (m_1 \dot{\tilde{x}}_1^2 + m_2 \dot{\tilde{x}}_2^2)$ where $\tilde{x}_1 = x_1 - x_d$. Using the same analysis as above we can obtain similar results as for the regulation.

3.2. Non-collocated regulation: limit cycles

The existence of clearance in this system breaks the kinematic chain and induces the creation of limit cycles (Choi and Noa, 1989). Its presence induced by the control law has been reported from numerical investigations in Azenha and Tenreiro Machado (1996). In this paper, we propose an analytical reasoning to prove the existence and stability of such limit cycles. The proposed technique is based on Kobrinskii's study of vibro-impact (Babitsky, 1998). This approach to finding the steady-state response for this forced piecewise linear system (Bapat et al., 1983; Masri and Caughey, 1966) reduces the problem to a set of nonlinear equations with boundary conditions. It consists of building the trajectories in the steady state using the knowledge of the solutions between collisions (the system is linear between impacts) and the impact law. We concatenate the solutions at the collision instants in order to obtain a complete solution. This formulation allows an implicit form of a three-dimensional Poincaré map and from this map we can obtain results about the stability of certain periodic motion. The Poincaré map used here is a map extensively used in the mechanical engineering literature for similar systems. Its formulation is based on the basic behavior of the system (the repetition of the collisions). For the analysis we consider only a special type of motion in order to simplify the calculations. The considered motion satisfies the following hypotheses: the limit cycle is symmetric, the periodic trajectory at steady state is only composed by backlash and collision phases (we exclude the trajectories considering contact phases) and there are only two collisions (one collision with each constraint) per period of the cycle. With the previous assumptions, we can build the solutions. Due to the supposed symmetry, only half of the trajectory needs to be considered. In considering only two collisions per period, the boundary conditions can be summarized by

$$\begin{aligned}
 x_{10} &\triangleq x_1(t_0^-) = x_{11} \triangleq x_1(t_0^+) = -x_1(t_1^-) \\
 x_{20} &\triangleq x_2(t_0^-) = x_{21} \triangleq x_2(t_0^+) = -x_2(t_1^-) \\
 y_{10} &\triangleq \dot{x}_1(t_0^-) = -y_{11} \triangleq -\dot{x}_1(t_0^+) = -\dot{x}_1(t_1^-) \\
 y_{20} &\triangleq \dot{x}_2(t_0^-) = -y_{22} \triangleq -\dot{x}_2(t_0^-)
 \end{aligned} \tag{11}$$

where t_0 is the instant of the first collision and $t_1 = t_0 + \Delta$ is the instant of the second collision. We denote Δ as the interval between two consecutive collisions. Because the cycle is built at the impact instant, $x_1(t_0^-) = x_2(t_0^-) + L$ and $x_1(t_1^-) = x_2(t_1^-) - L$. By resolving the system on the interval (t_0, t_1) the following expressions are obtained

$$\begin{aligned}
 x_1(t) &= x_{11} + y_{11}(t - t_0) \\
 y_1(t) &= y_{11} \\
 x_2(t) &= A_r + B_r(t - t_0) + C_r(t - t_0)^2 + D_r(t - t_0)^3 \\
 y_2(t) &= B_r + 2C_r(t - t_0) + 3D_r(t - t_0)^2
 \end{aligned} \tag{12}$$

where the constants of integration are given by

$$A_r = x_{21} \quad B_r = y_{21} \quad C_r = \frac{-k_p x_{11} - k_v y_{11}}{2m_2} \quad D_r = -\frac{k_p y_{11}}{6m_2}. \tag{13}$$

If the system equations (12) are evaluated at $t = t_1$ and the conditions of symmetry in equation (11) and the impact conditions are introduced, we obtain from equation (12) the time elapsed between two consecutive collisions given by $\Delta = -2\frac{x_{11}}{y_{11}}$. Algebraic manipulations allow us to show that the only limit cycle satisfying these hypotheses is characterized by (for the primary mass)

$$x_{10} = \frac{3Lm_2(1+e)^2k_v^2}{3(m_1+m_2)k_v^2(1+e)^2 - k_p(1-e)^2(m_1+m_2)^2} \quad (14)$$

$$y_{10} = \frac{x_{10}k_v(1+e)}{(m_1+m_2)(1-e)} \quad (15)$$

where x_{10} is the amplitude of the oscillation and y_{10} is the velocity of the primary mass at the collision instant. The position and velocity of the secondary mass are given such that the impact condition is satisfied.

3.2.1. Existence conditions

The solutions have a physical meaning and they must satisfy certain conditions. The first condition is that the sign of the post-impact relative velocity $y_r(t_k^+) = y_1(t_k^+) - y_2(t_k^+)$ depends on the attained constraint. In this case, the evaluation of the velocity gives a test which successfully eliminates the solutions without physical significance. Because of the symmetry, only the constraint $x_1 - x_2 = L$ will be considered, for which $\text{sgn}(y_r(t_k^+)) = -1$. After some calculations, we find $y_r(t_k^+) = -\frac{2e(1+\mu)}{1+e}y_{10}$, which implies $x_{10} > 0$. From equations (14) and (15) we obtain

$$k_v^2 > \frac{k_p}{3}(m_1+m_2) \left(\frac{1-e}{1+e} \right)^2. \quad (16)$$

Notice that the trajectory construction has been made at the collision instants only. Because these solutions are obtained by only regarding discrete instants, they do not yield the complete trajectory for arbitrary times. In particular, it is possible that certain solutions result in a relative displacement $x_r = x_1(t) - x_2(t)$ being larger than L during such time intervals. To account for such a physically impossible situation, the existence of the limit cycle requires the verification of the so-called *viability conditions*:

$$|x_1(t) - x_2(t)| \leq L \quad \forall t \in (t_0, t_1). \quad (17)$$

For the considered system, a *sufficient* condition for viability can be obtained. Indeed, viability conditions will be always satisfied if the relative velocity $y_r(\cdot)$ maintains constant sign on (t_0, t_1) (Babitsky, 1998). We have

$$y_r(t) = (y_{11} - B_r) - 2C_r(t - t_0) - 3D_r(t - t_0)^2 = a_0 + a_1\Delta I + a_2\Delta I^2. \quad (18)$$

Introducing the constants of integration, we obtain (considering $x_{10} > 0$) that $a_0 < 0$ and $a_2 < 0$. Given that $\Delta I = t - t_0 > 0$ a sufficient condition for viability is $a_1 < 0$. This is obtained if $C_r > 0$, which in turn is satisfied if

$$k_v^2 > k_p(m_1 + m_2) \left(\frac{1-e}{1+e} \right) \geq k_p(m_1 + m_2) \left(\frac{1-e}{1+e} \right)^2 \geq \frac{k_p}{3}(m_1 + m_2) \left(\frac{1-e}{1+e} \right)^2. \quad (19)$$

For the existence of the limit cycle, both equations (16) and (19) have to be satisfied simultaneously. Given that $1 \geq \frac{1-e}{1+e} \geq 0$, equation (19) is a sufficient condition for the existence.

3.2.2. Stability of the limit cycles

We study the stability of the limit cycles induced by the control law. Periodic orbits correspond to fixed points of the Poincaré map. In order to obtain a section to generate the Poincaré map P , we must have some knowledge of the geometrical structure of the phase space of the problem. For the considered system, it is possible to obtain a section relying on the insight of the system behavior. That is, the collisions take place when the two masses come in contact and the bodies move apart from each other after an impact. If the collision is repeated many times, the evolution of the system will be given by the system state evolution at the impact instants. This is a natural choice of the section given the nature of the system. It is important to observe that the discrete formulation of the Poincaré map enables us to eliminate the problem of discontinuities due to impacts.

To simplify the notation $z_1 = x_1$, $z_2 = y_1$, $z_3 = x_1 - x_2$ and $z_4 = y_1 - y_2$ are used. The geometry of the flow defined is $(z_1, z_2, z_4) \in \mathbb{R}^3$, z_3 is restricted to $I = [-L, L]$. The phase space defined is given by $(z_1, z_2, z_3, z_4) \in \mathbb{R}^2 \times I \times \mathbb{R}$. In systems of this type, there are two possibilities for the hypersurface defined by the collisions, one with each constraint. The intersections in the hypersurfaces are defined by the reduced state $(z_1, z_2, z_4) \in \mathbb{R}^3$. When a trajectory intersects the hypersurface it immediately jumps to another point on the hypersurface via the impact. This leaves four possible definitions of the Poincaré section. In the analysis, the pre-collision map with the constraint 1, $\Sigma_1^- = \{(z_1, z_2, z_3, z_4) | z_3 = L, z_4 > 0\} \in \mathbb{R}^2 \times I \times \mathbb{R}^+$, will be chosen arbitrarily for the calculations of stability. Because of the discontinuities, the Poincaré map must be constructed by composition of four simple mappings, defined as follows

$$P = P_{43} \circ P_{32} \circ P_{21} \circ P_{10} \quad (20)$$

where P_{10} and P_{32} correspond to the impact mappings whereas P_{21} and P_{43} correspond to the continuous flow. Note that P is known only in implicit form. Indeed, the solution of the time elapsed between impacts requires finding the roots of complicated polynomial equations. However, the behavior of the system can be characterized by the *local* stability of the fixed points. In order to determine the stability of a periodic solution emanating from $Z_0 = (z_{10}, z_{20}, z_{40})$, the Jacobian matrix of the Poincaré map P at Z_0 must be calculated. This derivative is obtained using implicit differentiation. The calculation of DP is carried out by considering the dynamics of small perturbations of the periodic solutions. Given the nature of the map, only the sensitivity matrix DP is known. The computation of DP must be decomposed into four parts to consider the contribution of each mapping

$$DP(z_{10}, z_{20}, z_{40}) = \frac{\partial P(z_{14}, z_{24}, z_{44})}{\partial(z_{10}, z_{20}, z_{40})} = DP_{43} DP_{32} DP_{21} DP_{10} \quad (21)$$

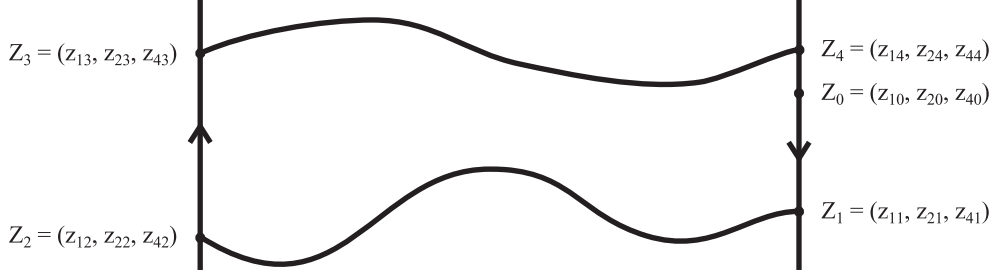


Figure 2. A schematic diagram of the flow in the phase plane.

where $DP_{ij} = \frac{P(z_{1i}, z_{2i}, z_{4i})}{(z_{1j}, z_{2j}, z_{4j})}$. In equation (21) DP_{21} comes from the free flight between the two constraints. The variables z_{12}, z_{22} and z_{42} are related to z_{11}, z_{21} and z_{41} by

$$\begin{aligned} g &\triangleq z_{32}(\Delta, z_{11}, z_{21}, z_{41}) = z_{11} + z_{21}\Delta - A_c - B_c\Delta - C_c\Delta^2 - D_c\Delta^3 = -L \\ f_1 &\triangleq z_{12}(\Delta, z_{11}, z_{21}, z_{41}) = z_{11} + z_{21}\Delta \\ f_2 &\triangleq z_{22}(\Delta, z_{11}, z_{21}, z_{41}) = z_{21} \\ f_3 &\triangleq z_{42}(\Delta, z_{11}, z_{21}, z_{41}) = B_c + 2C_c\Delta + 3D_c\Delta^2 \end{aligned} \quad (22)$$

where $\Delta = t_1 - t_0$ and A_c, B_c, C_c and D_c are given by

$$A_c = z_{11} - L \quad B_c = z_{21} - z_{41} \quad C_c = \frac{-k_p z_{11} - k_v z_{21}}{2m_2} \quad D_c = -\frac{k_p z_{21}}{6m_2}. \quad (23)$$

A calculation of implicit derivatives for the functions f_1, f_2, f_3 and g defined in equation (22) allows us to obtain $DP_{21} = \frac{P(z_{12}, z_{22}, z_{42})}{(z_{11}, z_{21}, z_{41})}$. The symmetry conditions imply $DP_{43} = DP_{21}$. Finally, we may compute that the characteristic polynomial of DP is given by

$$h_3 Z^3 + h_2 Z^2 + h_1 Z + h_0 \quad (24)$$

where the coefficients are given by

$$\begin{aligned} h_3 &= 9 \\ h_2 &= -4G^4 + 8(2+e)G^3 - 4(e^2 + 4e + 10)G^2 + 36(1+e)G - 9(1+2e^2) \\ h_1 &= 4G^4 - 8(1+2e)G^3 + 4(10e^2 + 4e + 1)G^2 - 36(1+e)e^2G + 9e^2(2+e^2) \\ h_0 &= -9e^4. \end{aligned} \quad (25)$$

Here $G \triangleq \frac{k_p(1-e)^2}{k_v^2(1+e)}(m_1 + m_2) \leq 1$ from equation (19). Using the Jury criterion,² it is easy to prove that the roots of the characteristic polynomial are always inside the unit circle provided that equation (19) holds. Therefore, we have proved the following:

Lemma 1. *Assume the non-collocated PD control is applied to the impact pair. Then if the condition in equation (19) is satisfied, a symmetric limit cycle described by equations (14) and (15) exists and is locally stable.*

Remark 2. *The stability of the fixed point of the Poincaré map, and the stability of the continuous-time trajectories, may in general be two different things. However, in the case of the system we deal with in this paper, they are equivalent due to the good properties of the continuous vector fields (which ensure that the existence, uniqueness and continuous dependence properties studied in Schatzman (1998) are satisfied).*

3.3. PD control: the tracking problem

In the previous section, we have seen that the existence and stability of limit cycles for the non-collocated regulation problem can be given a complete analytical solution. In this section, we choose $x_d(t)$ as a cosine function $x_d = x_m \cos \omega t$ so that U in equation (2) can be rewritten as

$$U = -k_v \dot{x} - k_p x + \beta \cos(\omega t + \zeta) \quad (26)$$

with $\beta \cos(\omega t + \zeta) = m_2 \ddot{x}_d + k_v \dot{x}_d + k_p x_d$. The amplitude and the phase are given by $\beta = x_m \sqrt{(k_p - m_2 \omega^2)^2 + (k_v \omega)^2}$ and $\tan \zeta = \frac{k_v \omega}{k_p - m_2 \omega^2}$.

Let us study the possible trajectories induced by the control law using the same method as in the previous subsection. We search for determined periodic orbits. More generally, the same type of analysis may be performed to try to prove the existence of any periodic orbit we desire to track exactly (in the ideal theoretical case). For instance, we may replace the sine function by a triangle or square periodic signal and proceed with a similar analysis to investigate whether some suitable orbits exist or not, although this problem is often untractable analytically in most cases. In this section, we outline the stability and existence analysis. More details can be found in Mata-Jiménez et al. (1997). Let us note that our analysis mainly departs from those in Babitsky (1998), Bapat et al. (1983), Heiman et al. (1987), Peterka and Vácik (1992) and Shaw and Rand (1989), in the sense that we focus our attention on the role played by the gains k_p and k_v , and we are not concerned with providing a zoological description (Hubbard and West, 1995, Section 7.6, p. 105) of the dynamics.

Let us denote the velocities of the primary and secondary masses as y_1 and y_2 , respectively. A periodic solution of order n will mean a solution which has a period n times the period of the control input $T = \frac{2\pi}{\omega}$ (where n is an integer). In the system there are many different types of periodic solutions of order n . However, in order to simplify the algebraic calculations only those periodic solutions that have a single impact with each of the boundaries during a single cycle will be taken into account (this is the simplest solution possible), referred to as *simple periodic solutions*. Finding the general solution is at best extremely difficult and Bapat et al. (1983) have demonstrated that the exact closed-form solutions are possible only when the number of collisions per period is equal to two. In this technique to find a simple periodic solution, it is assumed that the oscillator starts at the boundary $x_2 = x_{20}$ with initial velocity y_{20} . Only the symmetric periodic trajectories will be considered, and only the collocated control is analyzed for the sake of brevity. But some figures concerning the non-collocated case are presented for the sake of comparison and to enable us to draw some conclusions on the PD controller. Using Kobrinskii's method, we are able to prove the following (Mata-Jiménez et al., 1997):

Lemma 2. *Symmetric periodic orbits of order n exist only if the nonlinear equation*

$$(K_0^2 + \omega^2 L_0^2) y_{20}^2 - 2(L_0 J_0 \omega^2 x_{20}) y_{20} + \omega^2 J_0^2 (x_{20}^2 - x_m^2) = 0 \quad (27)$$

possesses a set of feasible solutions (x_{20}, y_{20}) where

$$x_m = \sqrt{\frac{(K_0^2 + \omega^2 L_0^2) y_{20}^2 - 2 \frac{L_0}{J_0} x_{20} y_{20} + x_{20}^2}{\omega^2 J_0^2}} \quad (28)$$

$$\begin{aligned} J_0 &= \cosh\left(\frac{nT\Omega}{2}\right) + \cosh\left(\frac{nT\rho}{2}\right) & \Omega &= \sqrt{\rho^2 - \frac{k_p}{m_2}} \\ L_0 &= \frac{1-R}{2\Omega} \sinh\left(\frac{nT\Omega}{2}\right) & \rho &= \frac{k_v}{2m_2} \\ K_0 &= \frac{1+R}{2} J_0 + \left(\frac{1-R}{2}\right) \left(\frac{\rho}{\Omega} \sinh\left(\frac{nT\Omega}{2}\right) + \sinh\left(\frac{nT\rho}{2}\right)\right) & R &= \frac{e+2\mu-1}{e-2\mu-1}. \end{aligned}$$

The orbits analyzed here correspond to $n = 2$. It is worth noting that, contrary to what is stated in Li et al. (1990) and Shaw and Rand (1989), the condition in equation (27) is not sufficient to guarantee the existence of a periodic trajectory. Indeed, the existence condition of the impact motion excludes the possibility of the occurrence of an additional impact during the time interval between the periodic impacts (Babitsky, 1998; Heiman et al., 1987; Peterka and Vacik, 1992). This can be expressed via the viability conditions as

$$|x_1 - x_2| < L \quad \text{for } t_0 < t < t_0 + \frac{nT}{2}. \quad (29)$$

In contrast to the non-collocated regulation case, the values of k_p and k_v satisfying the existence conditions can be obtained only numerically, as the process of obtaining them requires finding the roots of transcendental equations. The stability of the existing solutions can be analyzed similarly as for the non-collocated PD regulation case. This time, the geometry of the flow is given by $(z_1, z_2, z_4) \in \mathbb{R}^3$, φ is restricted to a circular phase S^T (the circle of period T) and z_3 is restricted to $[-L, L]$. The phase space is given by $(z_1, z_2, z_3, z_4, \varphi) \in \mathbb{R}^2 \times I \times \mathbb{R} \times S^T$.

As an illustration of the numerical results we may obtain, Figures 3(a) and 4(a) depict the domain in which there is at least one couple (k_p, k_v) such that for given (γ, w) (with $\gamma = \frac{L}{x_{10}}$ where x_{10} is the magnitude of the orbit, so that the form of the primary mass trajectory in the phase plane is fixed) the corresponding periodic solution exists. The existence regions correspond to the area above the depicted curves. Each curve corresponds to a particular couple (e, μ) . Figures 3(b) and 4(b) are constructed as follows. Given a point (γ, ω) on Figures 3(a) and 4(a) inside the existence region, we calculate all the possible couples (k_p, k_v) that give rise to a stable periodic trajectory. The couples (e, μ) in Figures 3(a) and 4(a) are the same.

Notice that:

- for a couple of physical parameters (e, μ) the desired trajectory may not exist;
- a different secondary mass trajectory corresponds to each couple (k_p, k_v) .

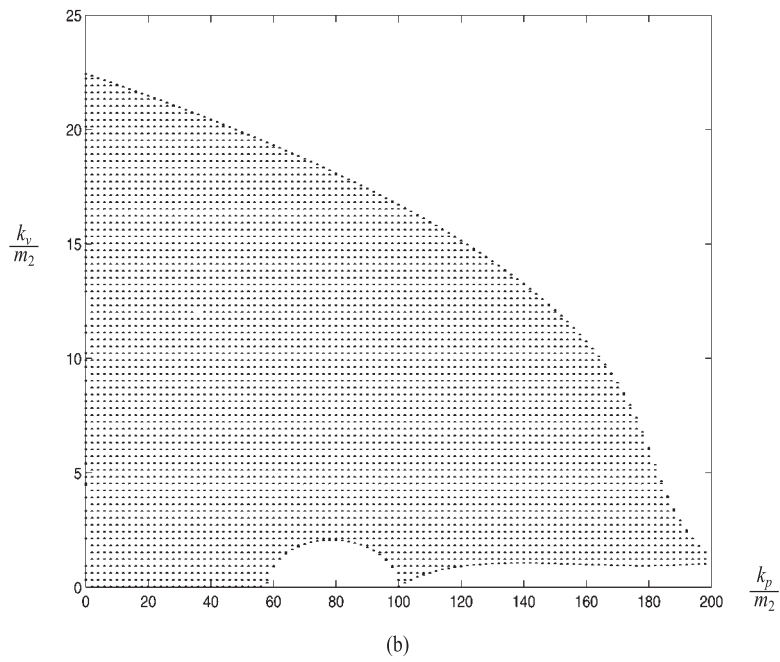
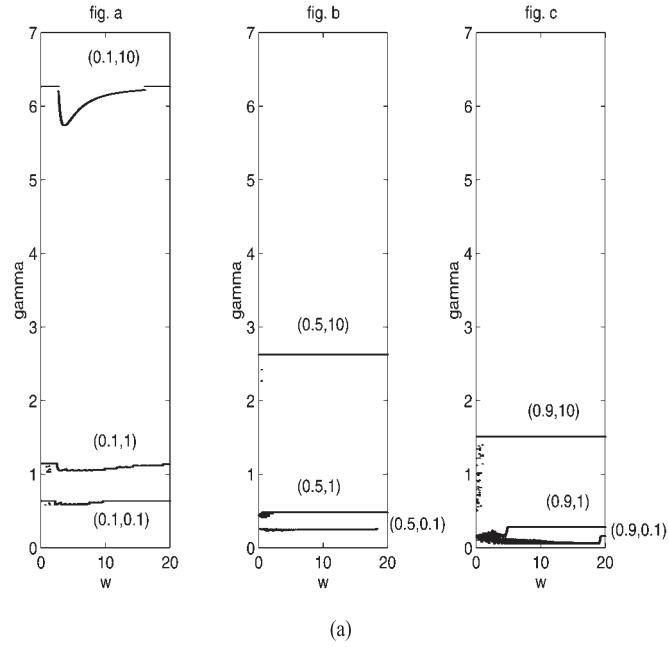
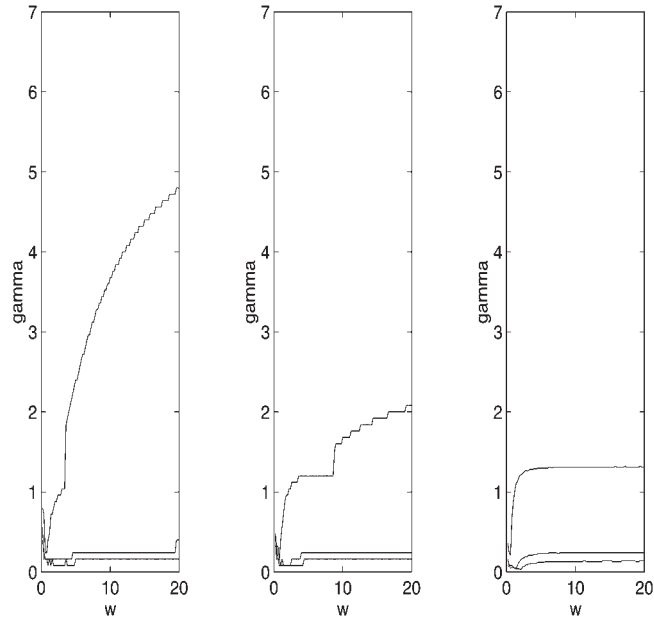
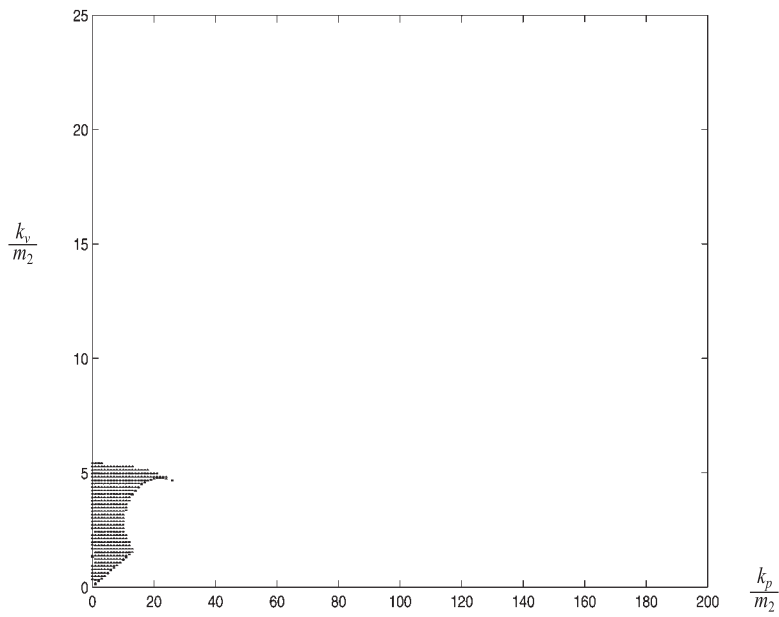


Figure 3. Collocated control: (a) existence areas as a function of (e, μ) ; (b) existence and stability areas as a function of (k_p, k_v) .



(a)



(b)

Figure 4. Non-collocated control: (a) existence areas as function of (e, m) ; (b) existence and stability areas as a function of (k_p, k_v) .

3.4. PD control: preliminary conclusions

From Mata-Jiménez et al. (1997) and the preceding analysis, it is possible to make the following conclusions about the performance we may expect from a PD controller:

- Regulation:
 - The collocated PD regulation guarantees global asymptotic stability properties.
 - In the non-collocated regulation case, we have proven analytically the existence of stable limit cycles.
- Tracking:
 - Some locally stable periodic orbits exist in a closed loop. The existence and stability regions are much smaller for the non-collocated case than for the collocated case, as expected.
 - For the non-collocated case, the region of existence and stability decreases with increasing e . It is the inverse for the collocated case.
 - The region of admissible gains is limited principally by the variation on $\gamma = \frac{L}{x_{10}}$.
 - The range of admissible gains corresponding to the chosen stable periodic trajectory is large for the collocated case. However, the desired trajectory of the primary mass may not exist.
 - Although the existence and stability regions for the non-collocated case are much smaller than for the collocated case, the basins of attraction have a similar size in both cases (Mata-Jiménez, 1998; Mata-Jiménez et al., 1997). However, in practice, the uncertainties on the physical parameters will be an obstacle to tracking, due to the high sensitivity of the basin of attraction size with respect to physical parameter uncertainties as shown in Mata-Jiménez (1998). This sensitivity is a classical feature of nonlinear systems (Grebogi et al., 1994).
 - It is clear that the PD control generally provides only local stability of the existing time-varying orbits. Moreover, the existing symmetric orbits constitute a very narrow class of trajectories, which may often lack of practical usefulness (because the magnitude is proportional to the clearance size in most of the cases). The proof of existence of other types of orbits (there may exist trajectories much closer to $x_d(t)$ than those we have investigated) always relies on heavy manipulations of nonlinear equations that have to be solved numerically.
 - Other types of desired signals $x_d(\cdot)$ can be considered in equation (5). However, the tracking performance is generally quite poor, as shown in numerical simulations at the end of the paper. In a general setting, even chaotic motions may be created (Shaw and Rand, 1989).
 - In practice, PD control strategies are stable for most desired motions; that is, closed-loop signals remain bounded. It can indeed be shown, using a reasoning inspired by Anglés (1996) and based on induction, that PD guarantees global boundedness of solutions when $x_d = \sin(\cdot)$. But again performance may be quite poor.

4. HYBRID CONTROL STRATEGY

Due to the limitations of a PD controller and the difficulties in obtaining analytical results concerning the existence of closed-loop stable time-varying trajectories, it is of interest to study other types of feedback controllers for the impact damper. This is the object of this section.

4.1. A general targeting control approach

We now present a general approach to targeting a desired point of the state space of the primary mass. Defining the elapsed time between two consecutive collisions as $\Delta_k = t_{k+1} - t_k$ we can obtain the system state just before the next collision for any control input $U \in \mathbb{R}$. If we assign ψ_1 as the change of the position, and ψ_2 as the change of the velocity due to the control, i.e. $\psi_1(t_k) = \int_{t_k}^{\tau} \int_{\tau}^{t_{k+1}} U d\tau d\xi$ and $\psi_2(t_k) = \int_{t_k}^{t_{k+1}} U d\tau$, then from equations (2) and (4) we can write the system as

$$\begin{aligned} x_1(t_{k+1}) &= x_1(t_k) + y_1(t_k^+) \Delta_k \\ x_2(t_{k+1}) &= x_2(t_k) + y_2(t_k^+) \Delta_k + \psi_1(t_k) \\ y_1(t_{k+1}^+) &= m_{11} y_1(t_k^+) + m_{12} y_2(t_k^+) + m_{12} \psi_2(t_k) \\ y_2(t_{k+1}^+) &= m_{21} y_1(t_k^+) + m_{22} y_2(t_k^+) + m_{22} \psi_2(t_k) \end{aligned} \quad (30)$$

where m_{ij} are the non-trivial entries of the matrix $\mathcal{E}(\mu, e)$ in equation (4) $i, j = 1, 2$ (i.e. $m_{11} = \frac{\mu - e}{1 + \mu}$ and so on). Note that we consider $\psi_1(t_k)$ and $\psi_2(t_k)$ independent and *a priori* arbitrary. If the system in equation (30) is not controllable a real system with a fixed structure $\psi_2 = f(\psi_1)$ cannot be. In addition, the viability conditions are not yet included at this stage of the study. They are investigated in detail in the next section. Therefore, the result in this subsection has to be considered necessary but not sufficient (in terms of impacts needed to attain the target). We note that equation (30) is not a simple discrete-time system due to the flight-time Δ_k in the first two equations. If we want to bring the trajectory from $X(t_k^+)$ to a desired state $X(t_{k+1}^+) = X^*(t_{k+1}^+)$, it is necessary to calculate the variation on the position, ψ_1 , and on the velocity, ψ_2 , to attain the target $(x_1(t_{k+1}), x_2(t_{k+1}), y_1(t_{k+1}^+), y_2(t_{k+1}^+)) = (x_1^*(t_{k+1}), x_2^*(t_{k+1}), y_1^*(t_{k+1}^+), y_2^*(t_{k+1}^+))$. Note, from equation (30), that we can reach the desired x_1 only indirectly using the flight time because the control input has no direct effect on its behavior. Then we select the interval between two consecutive collisions as

$$\Delta_k^* = \frac{x_1^*(t_{k+1}) - x_1(t_k)}{y_1(t_k^+)}. \quad (31)$$

Introducing equation (31) into equation (30) we obtain the system:

$$\begin{aligned} x_1^*(t_{k+1}) &= x_1^*(t_{k+1}) \\ x_2^*(t_{k+1}) &= x_2(t_k) + y_2(t_k^+) \Delta_k^* + \psi_1(t_k) \\ y_1^*(t_{k+1}^+) &= m_{11} y_1(t_k^+) + m_{12} y_2(t_k^+) + m_{12} \psi_2(t_k) \\ y_2^*(t_{k+1}^+) &= m_{21} y_1(t_k^+) + m_{22} y_2(t_k^+) + m_{22} \psi_2(t_k). \end{aligned} \quad (32)$$

From the above equations we deduce the following:

$$\begin{pmatrix} 1 & 0 \\ 0 & m_{12} \\ 0 & m_{22} \end{pmatrix} \begin{pmatrix} \psi_1(t_k) \\ \psi_2(t_k) \end{pmatrix} = \begin{pmatrix} x_2^*(t_{k+1}) - x_2(t_k) - y_2(t_k^+) \Delta_k^* \\ y_1^*(t_{k+1}) - m_{11} y_1(t_k^+) - m_{12} y_2(t_k^+) \\ y_2^*(t_{k+1}) - m_{21} y_1(t_k^+) - m_{22} y_2(t_k^+) \end{pmatrix}. \quad (33)$$

In a compact form this system can be written as

$$M\Psi_k = G(X^*(t_{k+1}^+), X(t_k^+)). \quad (34)$$

To solve equation (34) it is necessary that the desired state satisfies

$$G(X^*(t_{k+1}^+), X(t_k^+)) \in \text{Im}\{M\}. \quad (35)$$

If $e \in (0, 1]$ ($e = 0$ is a trivial case (Mata-Jiménez, 1998)) then equation (35) implies that the following condition is satisfied:

$$y_2^*(t_{k+1}^+) = \frac{m_{22}}{m_{12}} y_1^*(t_{k+1}^+) + \frac{m_{21}m_{12} - m_{11}m_{22}}{m_{12}} y_1(t_k^+). \quad (36)$$

If the condition in equation (36) is satisfied, we can rewrite the equation (33) as a reduced order mapping as

$$\begin{pmatrix} 1 & 0 \\ 0 & m_{12} \end{pmatrix} \begin{pmatrix} \psi_1(t_k) \\ \psi_2(t_k) \end{pmatrix} = \begin{pmatrix} x_2^*(t_{k+1}) - x_2(t_k) - y_2(t_k^+) \Delta_k^* \\ y_1^*(t_{k+1}) - m_{11} y_1(t_k^+) - m_{12} y_2(t_k^+) \end{pmatrix} \quad (37)$$

which can be expressed in compact form as

$$\bar{M}\Psi_k = \bar{G}(X^*(t_{k+1}^+), X(t_k^+)) \quad (38)$$

where $\bar{M} \in \mathbb{R}^{2 \times 2}$ is full rank. The system is invertible and has a solution depending on the desired state and the initial state:

$$\Psi_k^* = \Psi_k(X^*(t_{k+1}^+), X(t_k^+)). \quad (39)$$

Hence, in the closed loop, we obtain

$$G(X(t_{k+1}^+), X(t_k^+)) = M\Psi_k^* = G(X^*(t_{k+1}^+), X(t_k^+)) \quad (40)$$

which implies

$$X(t_{k+1}^+) = X^*(t_{k+1}^+). \quad (41)$$

Suppose we want to attain the target using only one collision, i.e. $X^c = X^*(t_{k+1}^+)$. Then, from equation (36) we can observe that, in general, the fixed point does not satisfy $G(X^c, X(t_k^+)) \in \text{Im}\{M\}$. This means that only one desired velocity can be obtained in one step.

To cope with this problem, we propose that an intermediate state (X^+) be attained between the initial state (X^i) and the target (X^c). The idea is to choose an intermediate state with an existence region that contains the initial state. Additionally, the intermediate state must be contained in the existence region of the target. The scheme consists of two steps:

- (i) in order to calculate X^+ , it is necessary to obtain the conditions such that X^c is attained in one collision, i.e.

$$y_1^+ = \left(\frac{m_{12} y_2^c - m_{22} y_1^c}{m_{21}m_{12} - m_{11}m_{22}} \right); \quad (42)$$

- (ii) to bring the initial state to X^+ , equation (36) must be satisfied in order that the existence region of X^+ contains X^i , i.e.

$$y_2^+ = \frac{m_{22}}{m_{12}} y_1^+ + \frac{m_{21}m_{12} - m_{11}m_{22}}{m_{12}} y_1^i. \quad (43)$$

From equations (42) and (43) we obtain the intermediate state

$$\begin{aligned} x_1^+, \quad x_2^+ \quad \text{such that} \quad |x_1^+ - x_2^+| = L \\ y_1^+ = \left(\frac{m_{12} y_2^c - m_{22} y_1^c}{m_{21}m_{12} - m_{11}m_{22}} \right) \\ y_2^+ = \frac{m_{22}}{m_{12}} y_1^+ + \frac{m_{21}m_{12} - m_{11}m_{22}}{m_{12}} y_1^i. \end{aligned} \quad (44)$$

Until now, we have only examined some general features of the system assuming we have an ideal equivalent control (ψ_1, ψ_2) at our disposal. In the next subsection, we propose two control laws U , which enable us to achieve the required task.

4.2. Constant-impulsive control

The first approach to targeting the desired fixed point consists of applying a constant control input at the impact time, and an impulsive input between two consecutive collisions to modify the velocity of the secondary mass. The algorithm is as follows. The primary mass starts in a constraint and a constant input λ_k is applied. The system evolves until an instant $t_i \in (t_k, t_{k+1})$, where an impulsive input p_k is applied to correct the velocity of the secondary mass. The procedure is applied as many times as necessary to reach the desired target (m is the number of times). In our formulation, we choose $m = 2$, see Remark 3 for more detail on whether such a choice is relevant or not. The equations describing the system between two consecutive impacts with the proposed control are (see equation (30))

$$\begin{aligned} x_1(t_{k+1}) &= x_1(t_k) + y_1(t_k^+) \Delta_k \\ x_2(t_{k+1}) &= x_2(t_k) + y_2(t_k^+) \Delta_k + \alpha_k p_k \Delta_k + \frac{\Lambda_k}{2} \Delta_k^2 \\ y_1(t_{k+1}^+) &= m_{11} y_1(t_k^+) + m_{12} y_2(t_k^+) + m_{12} \Delta_k \Lambda_k + m_{12} p_k \\ y_2(t_{k+1}^+) &= m_{21} y_1(t_k^+) + m_{22} y_2(t_k^+) + m_{22} \Delta_k \Lambda_k + m_{22} p_k \end{aligned} \quad (45)$$

where $\alpha_k = \frac{t_{k+1} - t_i}{\Delta_k}$ and $\Lambda_k = \frac{\lambda_k}{m_2}$. We choose the intermediate state as in equation (44). To bring the trajectory from the initial state to the intermediate state, the flight time is (see equation (31))

$$\Delta_k^* = \frac{x_1^+ - x_1^i}{y_1^i}. \quad (46)$$

Introducing equations (46) and (44) into equation (45) (as indicated in equation (37)) we can obtain a reduced controller form that brings the trajectory from the initial conditions to the intermediate state as a function of the discrete inputs Λ_k and p_k :

$$\begin{pmatrix} \frac{(\Delta_k^*)^2}{2} & \alpha_k \Delta_k^* \\ m_{12} \Delta_k^* & m_{12} \end{pmatrix} \begin{pmatrix} \Lambda_k \\ p_k \end{pmatrix} = \begin{pmatrix} x_2^+ - x_2^i - y_2^i \Delta_k^* \\ y_1^+ - m_{11} y_1^i - m_{12} y_2^i \end{pmatrix}. \quad (47)$$

Inverting the above equation, we obtain the control law on (t_k, t_{k+1}) :

$$\begin{pmatrix} \Lambda_k \\ p_k \end{pmatrix} = \begin{pmatrix} \frac{2(m_{12}(x_2^+ - x_2^i - \Delta_k^* y_2^i) - \alpha_k \Delta_k^* (y_1^+ - m_{11} y_1^i - m_{12} y_2^i))}{m_{12} (\Delta_k^*)^2 (1 - 2\alpha_k)} \\ \frac{2m_{12}(x_2^+ - x_2^i - \Delta_k^* y_2^i) - \Delta_k^* (y_1^+ - m_{11} y_1^i - m_{12} y_2^i)}{m_{12} \Delta_k^* (2\alpha_k - 1)} \end{pmatrix} \quad (48)$$

In the second step, the system is considered on (t_k, t_{k+2}) . From equation (31), $x_1(t_{k+2}) = x_1^c$ implies

$$\Delta_{k+1}^* = \frac{x_1^c - x_1^+}{y_1^+}. \quad (49)$$

To obtain the values for the control inputs, we proceed as in the previous step. It follows from the above choices of intermediate target that y_1^* and y_2^* are achieved simultaneously. We obtain

$$\begin{pmatrix} \Lambda_{k+1} \\ p_{k+1} \end{pmatrix} = \begin{pmatrix} \frac{2(m_{12}(x_2^c - x_2^+ - \Delta_{k+1}^* y_2^+) - \alpha_{k+1} \Delta_{k+1}^* (y_1^c - m_{11} y_1^+ - m_{12} y_2^+))}{m_{12} (\Delta_{k+1}^*)^2 (1 - 2\alpha_{k+1})} \\ \frac{2m_{12}(x_2^c - x_2^+ - \Delta_{k+1}^* y_2^+) - \Delta_{k+1}^* (y_1^c - m_{11} y_1^+ - m_{12} y_2^+)}{m_{12} \Delta_{k+1}^* (2\alpha_{k+1} - 1)} \end{pmatrix}. \quad (50)$$

The above developments lead us to assume that there is no impact on the intervals (t_k, t_{k+1}) and (t_{k+1}, t_{k+2}) . Conditions on t_i , i.e. on α_k , are given next that guarantee the viability of the controller, so that the target can effectively be attained in two steps. A controller will be called viable if the corresponding closed-loop solution is viable as defined in the previous section (in other words there are no ‘‘accidental’’ or unwanted impacts).

4.2.1. Calculation of suitable impulse instants t_i (viability conditions)

The conditions given by equation (60) in the Appendix can be translated as the election of the switching instant α_k . The flight between the two constraints can be divided into two phases. The two phases will be considered independently. On (t_k, t_i) , the flight time between two collisions is given by

$$\Delta_{ph1}^2 \frac{\Lambda_k}{2} + (y_2(t_k^+) - y_1(t_k^+)) \Delta_{ph1} + (x_2(t_k) - x_1(t_k)) = x_2(t_p) - x_1(t_p) \quad (51)$$

where $\Delta_{ph1} = t_p - t_k$, t_p is the possible impact time (undesired) and $(x_2(t_p) - x_1(t_p))$ is the constraint of the unwanted collision. If $t_p > t_i$ (which will be satisfied if α_k and the inputs are suitably chosen, as shown later), the flight time between the constraints is given by

$$\Delta_k^2 \frac{\Lambda_k}{2} + (\alpha_k p_k + y_2(t_k^+) - y_1(t_k^+)) \Delta_k + (x_2(t_k) - x_1(t_k)) = x_2(t_{k+1}) - x_1(t_{k+1}). \quad (52)$$

Equations (51) and (52) are quadratic. With the two constraints, each provides four different solutions depending on the impact constraints. It is notable that the form of the solution is given by the value of the inputs Λ_k and p_k . If we use the criterion of the flight time, it is possible to choose the impact constraint with an adequate selection of Λ_k and p_k . In this physical configuration, there is always a solution. With this criterion, we can state the conditions for the non-existence of time t_p :

$$\Delta_{ph1} > \alpha_k \Delta_k \quad (53)$$

$$\Delta_k = \Delta_k^*. \quad (54)$$

The condition in equation (53) expresses that the solution of equation (51) is larger than the interval (t_k, t_i) . The condition in equation (54) means that the only solution of equation (52) (assuming that equation (53) is true) is the desired flight time. The two equations displayed above are functions of α_k . We can simply find numerically the range of α_k satisfying these conditions. This procedure must be applied to the two steps of the algorithm. In Appendix 5 we outline the way viability conditions can be analyzed.

Remark 3. (global basin of attraction) If there were no unilateral constraints, it would be possible to obtain the target in two steps from any initial condition, i.e. $m = 2$. However, the viability conditions imply a particular choice of the impulse instant t_i (i.e. of α_k), which reduces the size of the closed-loop basin of attraction. It is clear that, if B_m denotes the basin of attraction for the control with m impacts, then $B_{m+1} \supseteq B_m$. We have the following:

Lemma 3. *Consider the dynamics in equations (2)–(4) and a constant–impulsive input in equations (48) and (50). Then, if $\alpha_k \rightarrow 0$, $\alpha_k > 0$ and if the initial velocity $y_1(t_k^+) > 0$, the control is viable whatever the initial and target states, and the target is (in the ideal theoretical setting) attained after two impacts.*

The proof is given in Appendix B.

This is an interesting result as it shows that, in practice, we may enlarge the basin of attraction by modifying certain control parameters. One direction of future investigations is to increase the number of impacts, m , necessary to attain the target in order to comply with input magnitude or/and with viability constraints. This has been studied for a one-degree-of-freedom juggler to decrease the input in Zavala Río and Brogliato (1999). In practice, we expect that $m > 2$ will be needed in general to obtain a good performance of the controller.

4.3. Piecewise constant input control

The strategy in the previous subsection uses an impulsive input, which is a drawback in practice. It is therefore of interest to show that other controllers can be designed. This second control brings the trajectory on the basin of attraction around the fixed point using a constant input at the collision time and another constant input (with different amplitude) between two consecutive impacts. The algorithm can be summarized as follows. The primary mass starts in a constraint and a constant input λ_k is applied. The system evolves until an instant $t_i \in (t_k, t_{k+1})$ where the input amplitude is changed to γ_k . The procedure is applied as many times as necessary to reach the fixed point (as in the preceding section, m denotes this number of times). The equations governing the system between two consecutive impacts with the piecewise constant control are

$$\begin{aligned}
x_1(t_{k+1}) &= x_1(t_k) + y_1(t_k^+) \Delta_k \\
x_2(t_{k+1}) &= x_2(t_k) + y_2(t_k^+) \Delta_k + \frac{\Lambda_k \Delta_k^2}{2} (1 - \alpha_k^2) + \frac{\Gamma_k}{2} \Delta_k^2 \alpha_k^2 \\
y_1(t_{k+1}^+) &= m_{11} y_1(t_k^+) + m_{12} y_2(t_k^+) + m_{12} \Lambda_k (1 - \alpha_k) \Delta_k + m_{12} \Gamma_k \alpha_k \Delta_k \\
y_2(t_{k+1}^+) &= m_{21} y_1(t_k^+) + m_{22} y_2(t_k^+) + m_{22} \Lambda_k (1 - \alpha_k) \Delta_k + m_{22} \Gamma_k \alpha_k \Delta_k \quad (55)
\end{aligned}$$

where $\Lambda_k = \frac{\lambda_k}{m_2}$ and $\Gamma_k = \frac{\gamma_k}{m_2}$. Let us choose the intermediate state as in equation (44). To bring the trajectory from the initial state to the intermediate state, the flight time is as in equation (46). Introducing equations (46) and (44) into equation (55) (as indicated in equation (37)) we can obtain a reduced controller form that brings the trajectory from the initial conditions to the intermediate state as a function of the discrete inputs Λ_k and Γ_k :

$$\begin{pmatrix} \frac{(\Delta_k^*)^2(1-\alpha_k^2)}{m_{12}\Delta_k^*} & \frac{\alpha_k^2(\Delta_k^*)^2}{2\Delta_k^*} \\ m_{12}\Delta_k^*(1-\alpha_k) & \alpha_k m_{12}\Delta_k^* \end{pmatrix} \begin{pmatrix} \Lambda_k \\ \Gamma_k \end{pmatrix} = \begin{pmatrix} x_2^+ - x_2^i - y_2^i \Delta_k^* \\ m_{12}y_1^+ - m_{11}y_1^i - m_{12}y_2^i \end{pmatrix}. \quad (56)$$

Inverting equation (56) we can obtain the control law on (t_k, t_{k+1}) :

$$\begin{pmatrix} \Lambda_k \\ \Gamma_k \end{pmatrix} = \begin{pmatrix} \frac{2m_{12}(x_2^+ - x_2^i - y_2^i \Delta_k^*) - \alpha_k \Delta_k^* (y_1^+ - m_{11}y_1^i - m_{12}y_2^i)}{m_{12}(\Delta_k^*)^2(1-\alpha_k)} \\ \frac{-2m_{12}(x_2^+ - x_2^i - y_2^i \Delta_k^*) + (1+\alpha_k)(y_1^+ - m_{11}y_1^i - m_{12}y_2^i)}{m_{12}(\Delta_k^*)^2 \alpha_k} \end{pmatrix}. \quad (57)$$

In the second step, the system is considered on (t_k, t_{k+1}) . From equation (31), $x_1(t_{k+2}) = x_1^c$ implies equation (49). To obtain the values for the control inputs, we proceed as in the previous step. It follows from the above choices of intermediate target that y_1^* and y_2^* are achieved simultaneously. We obtain

$$\begin{pmatrix} \Lambda_{k+1} \\ \Gamma_{k+1} \end{pmatrix} = \begin{pmatrix} \frac{2m_{12}(x_2^c - x_2^+ - y_2^+ \Delta_{k+1}^*) - \alpha_{k+1} \Delta_{k+1}^* (y_1^c - m_{11}y_1^+ - m_{12}y_2^+)}{m_{12}(\Delta_{k+1}^*)^2(1-\alpha_{k+1})} \\ \frac{-2m_{12}(x_2^c - x_2^+ - y_2^+ \Delta_{k+1}^*) + (1+\alpha_{k+1})(y_1^c - m_{11}y_1^+ - m_{12}y_2^+)}{m_{12}(\Delta_{k+1}^*)^2 \alpha_{k+1}} \end{pmatrix}. \quad (58)$$

Notice that the inputs in equations (57), (58) and (48), (50) are similar but not equal. The viability conditions have to be checked in the same way as for the constant–impulsive input. As long as the basin of attraction is not the whole state space, it is clear that we will need $m > 2$ to attain the target point. In contrast to the constant–impulsive control, a numerical study will be needed to determine the basin of attraction as a function of m and the initial and target states.

Remark 4. It can be easily shown that defining a third magnitude modification between two impacts is useless in terms of controllability of the system, as shown in the previous subsection, although viability conditions may require $m > 2$ in general. An open problem is to determine the reachable space within m impacts, in an analytical way.

4.4. A hybrid PD + controller

In this subsection, we illustrate how the above targeting controller can be used in conjunction with a PD input to assure tracking of some important classes of desired orbits. The basic principle of this scheme is simple. We use the property of the collocated PD that ensures not

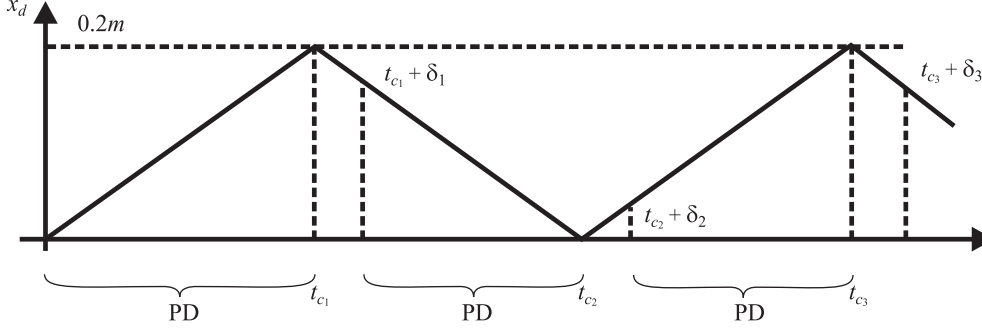


Figure 5. PD+ strategy.

only global regulation (i.e. stability of the invariant set in equation (7)), but also possesses some tracking capabilities when $\text{sgn}(\dot{x}_d(t))$ remains constant. We consider the example of a triangle signal with a period of 1 s. The proposed hybrid PD+ controller merely consists of switching from the PD to a targeting (constant–impulsive or piecewise constant) input when the slope of x_d changes, at times t_{c_i} and on the interval $[t_{c_i}, t_{c_i} + \delta_i]$, with $\delta_i = 0.05s$ (see Figure 5).

The goal is to compare the performance of the PD and the PD+ controllers according to the two criteria:

$$\begin{aligned}
 C_1 & : \int_{\text{period}} [(x_1 - x_d)^2 + (\dot{x}_1 - \dot{x}_{1d})^2 + U^2] d\tau, \\
 C_2 & : \int_{\text{period}} [(x_1 - x_d)^2 + (\dot{x}_1 - \dot{x}_{1d})^2] d\tau. \tag{59}
 \end{aligned}$$

In the following, the piecewise constant input has been used and the intermediate states are computed such that they minimize the distance to the target, taking into account viability conditions at each step. In the presented examples, we have not taken into account the viability conditions. In other words, if the controller is not viable, then an accidental impact occurs. In addition, only two intermediate points have been chosen. Consequently, it is clear that adding more intermediate points and incorporating the viability constraints could have been used as another control parameter, which would have enabled us to improve the results concerning the PD+ input (both the tracking performance and the input magnitude). Due to the high number of control parameters and to the high nonlinearity of the process, obtaining general results seems hopeless. We have therefore preferred to limit ourselves to some typical values of the parameters μ and $\frac{L}{A}$, but we have made the restitution coefficient e vary in $[0, 1]$. Notice also that the figures are presented from normalized dynamics, and can therefore be used for a large variety of parameters L and A .

First, note that there is no general procedure to choose the PD gains in an optimal way for such a system. Consequently, we have chosen an arbitrary couple $(k_p, k_v) = (23, 45)$ for the PD so that our results remain more qualitative than quantitative at this stage.

- Robustness of the PD+: From Figures 6(B) and (D) and from Figure 8, we see that, despite an uncertainty $\frac{\Delta e}{e} = 0.15$ on the restitution coefficient, the tracking performances of the PD+ are still better than those of the PD, for all values of $e \in [0, 1]$, and various values of μ and $\frac{L}{A}$.
- Input magnitude:
From Figures 6(A) and (C) and from Figure 8(C) we deduce that the control magnitude is larger for the PD+ than for the PD, in general. However, the results in Figures 7(A)–(D) contradict this conclusion. We should keep in mind that the high nonlinearity of the model prevents us from drawing very general conclusions, and that some irregular behavior in the dynamics is possible. Figure 10 illustrates the influence of e on the shape of the input U ; when e is close to 0 (plastic impacts), then the overall system (and consequently U) behaves much more nicely (less impacts) than when e is closer to 1. From Figures 6 and 7, we see that, as $\frac{L}{A}$ decreases, then C_1 decreases for the PD+ whereas C_1 remains constant for the PD input (recall that the values of the vertical axis have to be multiplied by $\frac{1}{L^2}$, i.e. the vertical scale of Figure 7 has to be multiplied by 10^{-4} to be compared with Figure 6).
- Sensitivity with respect to e : In Figure 9 we illustrate the sensitivity of the motion with respect to variations on e , as Figures 6(C), 8(B) or 9(A) show. The peak around $e = 0.8$ in Figure 9(A) can be explained from the phase plane orbits in Figures 9(B) and (C) (Figure 9(C) is a zoom of Figure 9(B)). Indeed, we see that changing e from 0.8 to 0.85 (i.e. 6.25%) modifies significantly the orbits of the system, and consequently modifies the values of the criteria C_1 and C_2 . This again is an illustration of the high nonlinearities of the system in equation (2).
- Importance of U in C_1 : From Figures 6(A)–(D), 7(A)–(D) and 8(A)–(D), it is clear that the contribution of U^2 in the criterion C_1 is larger with respect to the contribution of the tracking error squares. This is the case for both the PD and the PD+ controls.
- Influence of e on the number of impacts: The results of Figure 10 prove that such impacting systems behave better when e is close to 0, than when e increases, since the number of impacts decreases significantly as e decreases (the jumps in U correspond to shocks). This also shows that the increasing values of C_1 and C_2 in Figures 6(A), 7 and 8, are due to the increasing number of impacts in the system. However, depending on μ and $\frac{L}{A}$, this may be contradicted (see Figures 6(C) and 9(A)).
- Tracking capabilities of the PD+ control: From Figures 6(B) and (D), and 7(C) and (D), it is clear that the action of the discrete control when the motion reverses, drastically improves the tracking performance of the PD control (at least when all the parameters are known).
- Conclusions: The PD+ input improves the tracking performance of the PD input, and presents interesting robustness properties with respect to uncertainties on e . However, this is at the price of a generally larger control magnitude. These numerical results only aim at showing some typical tendencies of the closed-loop behavior, for some values of the parameters μ and $\frac{L}{A}$. They also show that, as expected, the non-smooth model is quite nonlinear and results may be quite sensitive to small variations of physical or control parameters. This, however, reflects the physical behavior of such systems which require specific tools for their analysis and control. An interesting conclusion

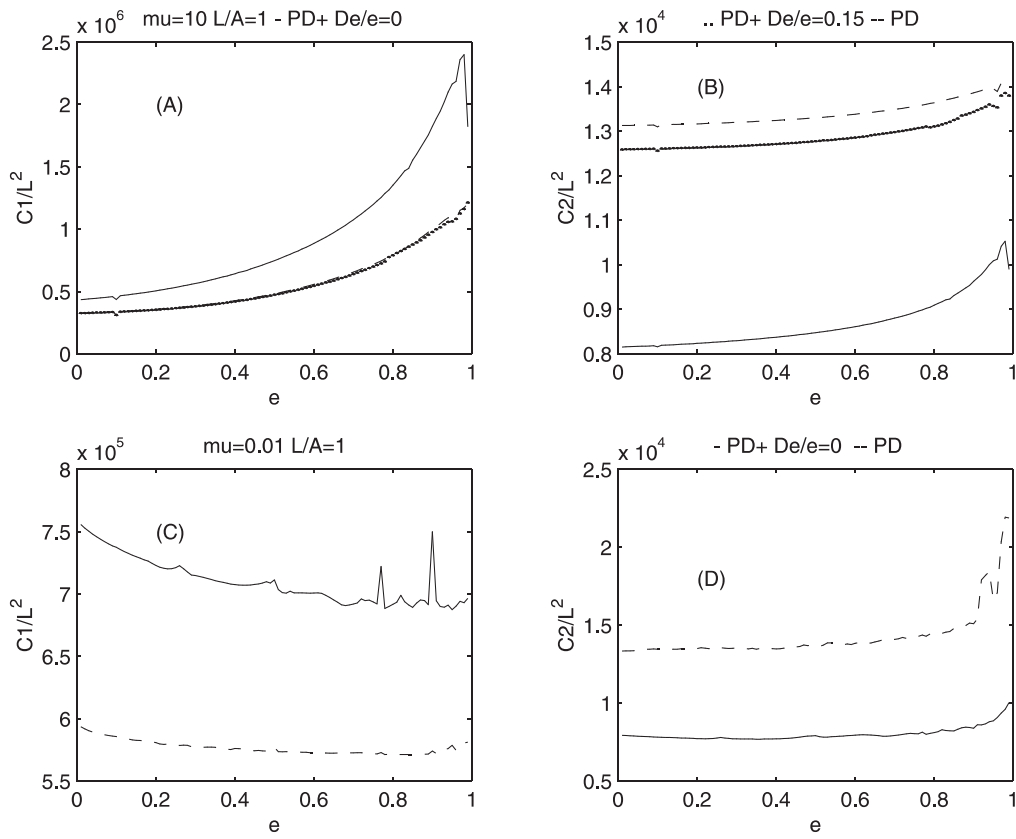


Figure 6. Criteria C_1 and C_2 (PD+ with $\frac{\Delta e}{e} = 0$ and $\frac{\Delta e}{e} = 0.15$ and PD).

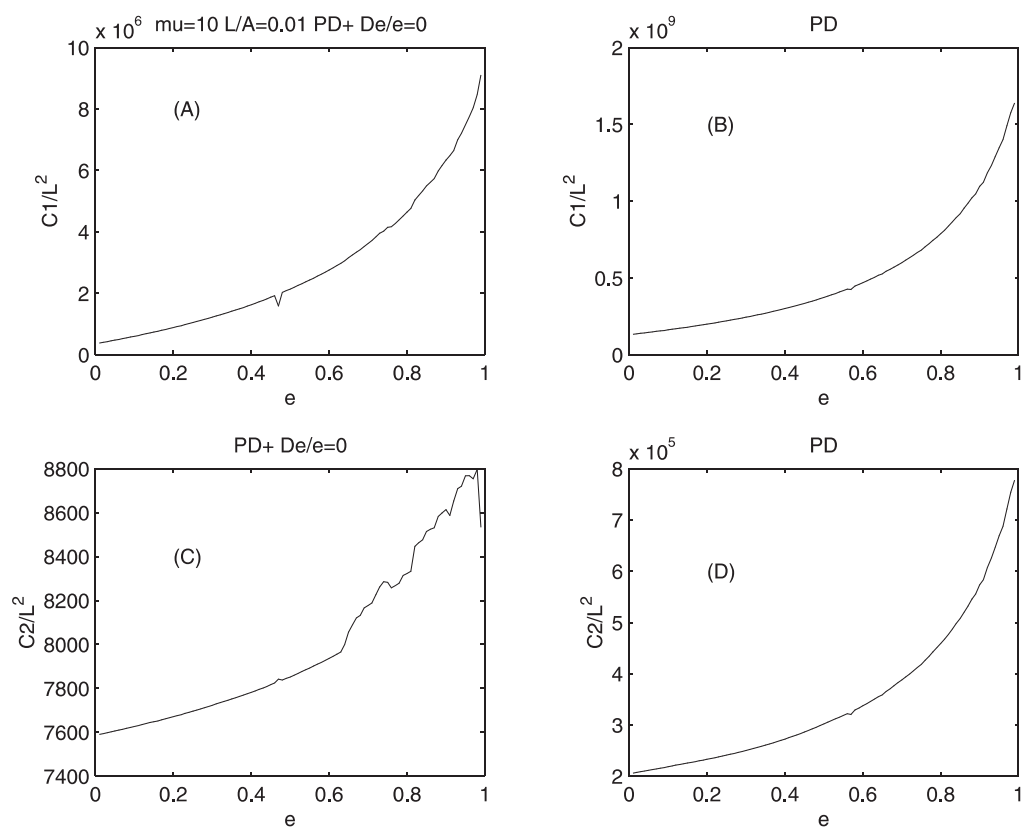


Figure 7. Criteria C_1 and C_2 (PD+ with $\frac{\Delta e}{e} = 0$ and $\frac{\Delta e}{e} = 0.15$ and PD).

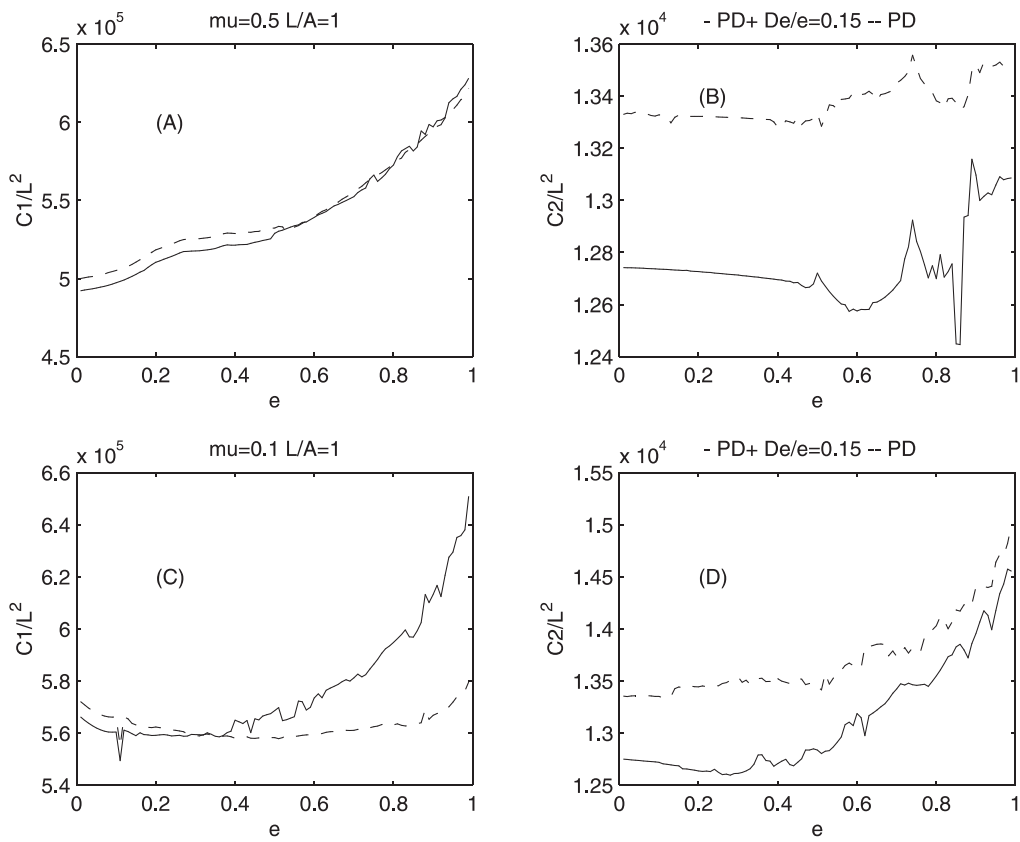


Figure 8. Criteria C_1 and C_2 (PD+ with $\frac{\Delta e}{e} = 0$ and $\frac{\Delta e}{e} = 0.15$ and PD).

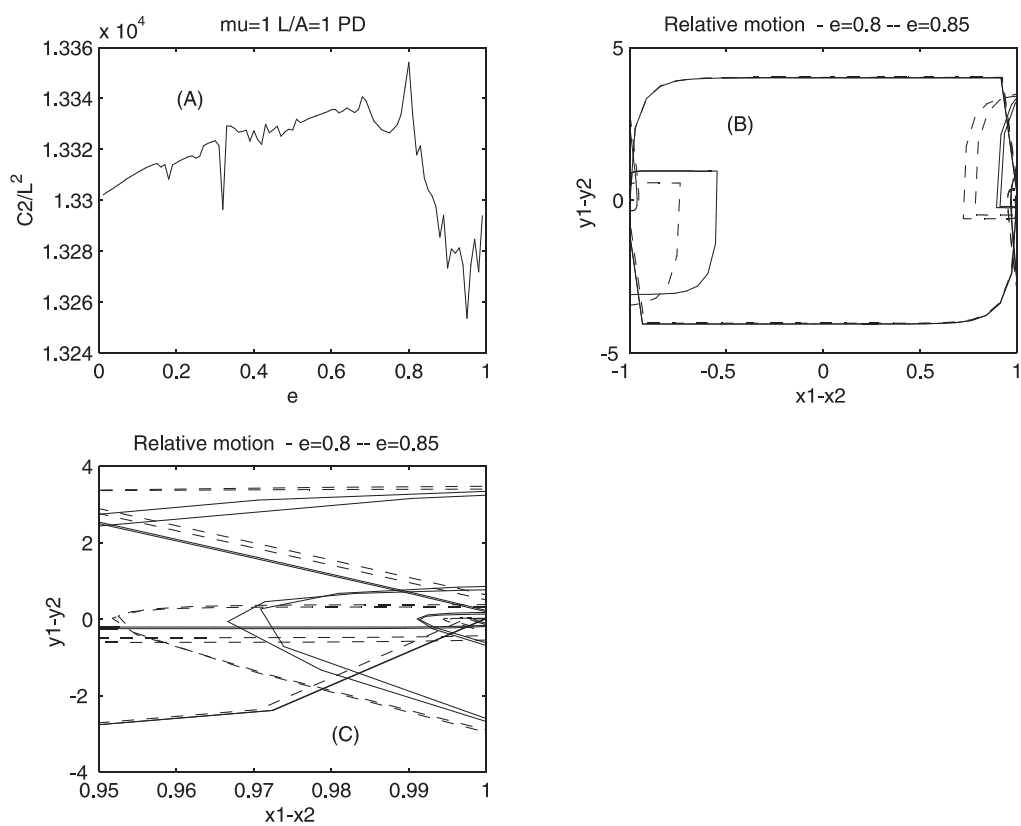


Figure 9. Criterion C_2 and relative motion (PD control).

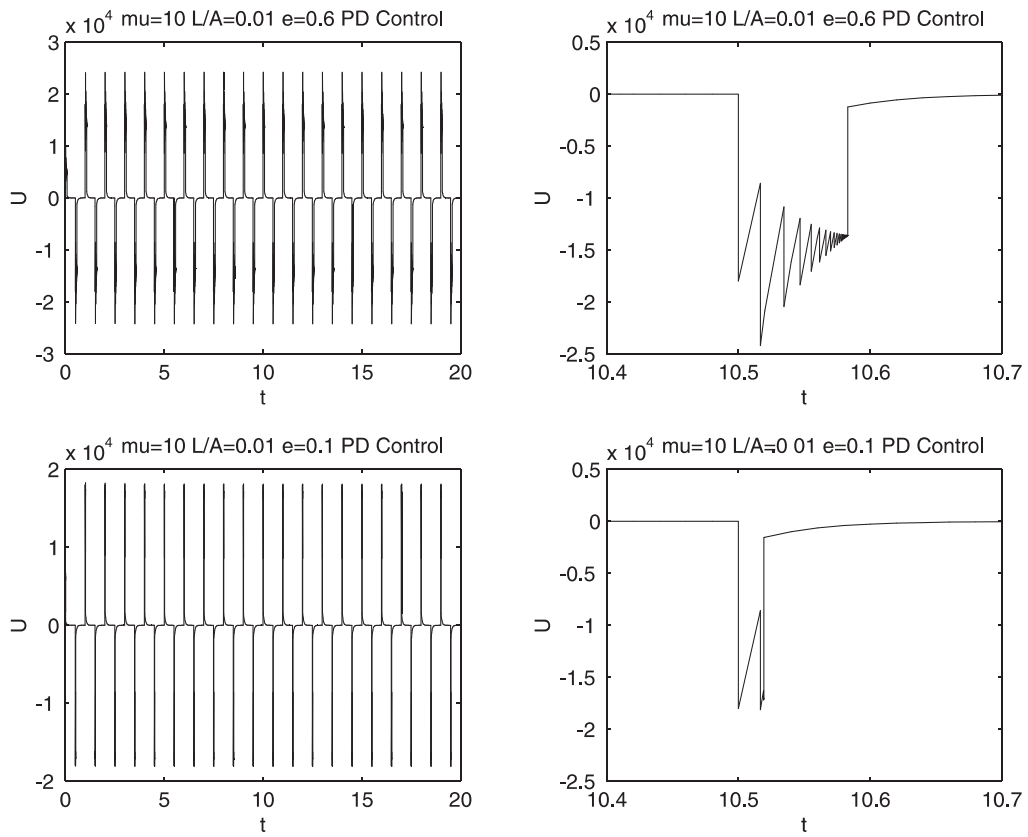


Figure 10. Control input (PD control).

is also that plastic impact ($e = 0$) generally facilitates the control of an impacting pair; because it dissipates more energy and decreases the number of impacts involved in the closed-loop system.

We have normalized the dynamical equations as follows: $X = \frac{x}{L}$, $\tau = \frac{t}{T}$. The simulations were realized in the normalized system. In other words, the presented graphs in Figures 6–10 can be read for any couple (L, A) .

Remark 5. (Neglected dynamics) *It is noticeable that the introduction of viscous friction terms ($\pm f(\dot{x}_1 - \dot{x}_2)$) in equation (2) allows us to put the free-motion dynamics into a triangular form. However, specific techniques such as backstepping do not seem promising because they do not simplify the dynamics of the primary mass during backlash phases. A more promising path consists of applying a simple control U (like those above), then deducing $\dot{q}_2(t)$ on backlash phases and introducing this function of time into the primary mass dynamics. Then, integration of these dynamics is possible to obtain $q_1(t)$ and $\dot{q}_1(t)$ as explicit functions of time, and the analysis can be recast into the framework developed in this paper.*

5. CONCLUSIONS

In this paper, the control of mechanical systems with backlash has been attacked via the study of the so-called impact damper. Despite its apparent simplicity, this system incorporates most of the basic dynamical effects encountered in such non-smooth hybrid dynamical systems. This system belongs to the class of complementary-slackness mechanical systems (Brogliato, 1999; Lötstedt, 1982). We have first studied the closed-loop behavior of PD controls, and then of a nonlinear switching scheme. The proposed hybrid control strategy is a simple feedback controller that enables us to bring the primary mass from one point of its state space to another. It can be used in conjunction with a PD control to improve its tracking capabilities. It finds potential applications in:

- (i) enlarging the basin of attraction and accelerating the convergence rate of locally stable orbits with PD controls;
- (ii) tracking a pre-specified sequence of states defined at impact times;
- (iii) controlling the change of direction of motion to track certain time-varying orbits in order to keep both masses stuck together during the phases with constant velocity.

It is notable that item (iii) allows us to derive controllers which are close in spirit to those in Tao and Kokotovic (1995), i.e. keeping the two masses stuck together despite a possible change of direction in the motion. However, the consideration of dynamical and impact effects renders the analysis quite different from those based on a hysteresis model.

The robustness issues are particularly important. Some numerical results show that the hybrid PD+ controller presents reasonable robustness properties with respect to uncertainties on the restitution coefficient e . Some applications carried out elsewhere (Fanuc, 1994; Chalhoub and Zhang, 1996) prove that it is quite possible in practice to detect the backlash phases and apply some switching strategies depending on the variation of the system topology. Future research will focus first on the experimental validation of the various results presented in this paper. Then, it would be of interest to study the extension of the hybrid control to nonlinear kinematic chains using nonlinear control schemes in conjunction with the piecewise

constant input, and on the study of the relationships between viability, reachable spaces in m impacts and robustness. In practice, such control strategy may be coupled with an on-line estimation software (Podsedkowski, 1997) to update the clearance parameters when the PD+ performance decreases below some threshold. Also, the control of liquid slosh in fuel tanks (Ibrahim and Sayad, 1998; Pilipchuk and Ibrahim, 1997; Hung and Pan, 1996) deserves attention.

APPENDIX A.

VIABILITY CONDITIONS FOR THE TARGETING CONTROL

The design of the controls has been made without regarding the viability conditions. Because the controllers are obtained only addressing the discrete state of the collision, they do not yield the complete trajectory for arbitrary times between two consecutive collisions. In particular, it is possible that certain solutions induced by the control result in a relative displacement violating the physical restrictions $h(q) \geq 0$. In this appendix, we give the criterion to eliminate non-viable inputs. Suppose that the limit of the viability conditions can be represented in the compact form

$$P(X(t_k^+), U_k, \Delta_k^*) = 0 \quad (60)$$

where Δ_k^* is the desired flight-time programmed in the controller. Note that the structure of equation (60) depends on the used control. In general, the resolution of equation (60) is not single valued, given certain initial conditions and control. However, it is possible to use the physical significance of the time Δ_k to disambiguate the multiple solutions. Indeed, Δ_k can be obtained by finding the minimal time satisfying the condition in equation (60), i.e.

$$\Delta_k = \inf\{\Delta > 0 | P(X(t_k^+), U_k, \Delta) = 0\}. \quad (61)$$

The controller is viable if $\Delta_k = \Delta_k^*$ and is not if $\Delta_k < \Delta_k^*$.

The initial constraint is $x_1 - x_2 = L$

Applying this criterion to the constant input Λ_k , we find after some lengthy calculations the following results that allow us to calculate the interval Δ_{ph1} in equation (51):

$$\Delta_{ph1} = \begin{cases} \frac{y_1(t_k^+) - y_2(t_k^+) + \sqrt{(y_1(t_k^+) - y_2(t_k^+))^2 + 4L\Lambda_k}}{\Lambda_k} & \text{if } \Lambda_k \geq -\frac{(y_1(t_k^+) - y_2(t_k^+))^2}{4L} \\ \frac{2(y_1(t_k^+) - y_2(t_k^+))}{\Lambda} & \text{if } \Lambda_k < -\frac{(y_1(t_k^+) - y_2(t_k^+))^2}{4L} \end{cases} \quad (62)$$

$$x_1(t_p) - x_2(t_p) = \begin{cases} -L & \text{if } \Lambda_k \geq -\frac{(y_1(t_k^+) - y_2(t_k^+))^2}{4L} \\ L & \text{if } \Lambda_k < -\frac{(y_1(t_k^+) - y_2(t_k^+))^2}{4L} \end{cases} \quad (63)$$

The initial constraint is $x_1 - x_2 = -L$

$$\Delta_{ph1} = \begin{cases} \frac{y_1(t_k^+) - y_2(t_k^+) - \sqrt{(y_1(t_k^+) - y_2(t_k^+))^2 - 4L\Lambda_k}}{\Lambda_k} & \text{if } \Lambda_k \geq -\frac{(y_1(t_k^+) - y_2(t_k^+))^2}{4L} \\ \frac{2(y_1(t_k^+) - y_2(t_k^+))}{\Lambda} & \text{if } \Lambda_k < -\frac{(y_1(t_k^+) - y_2(t_k^+))^2}{4L} \end{cases} \quad (64)$$

$$x_1(t_p) - x_2(t_p) = \begin{cases} -L & \text{if } \Lambda_k \geq -\frac{(y_1(t_k^+) - y_2(t_k^+))^2}{4L} \\ L & \text{if } \Lambda_k < -\frac{(y_1(t_k^+) - y_2(t_k^+))^2}{4L} \end{cases}. \quad (65)$$

The same type of expressions can be obtained for Δ_k in equation (52). When $\alpha_k \rightarrow 0$, it is clear from equation (52) that the expressions are even equal.

APPENDIX B.

PROOF OF LEMMA 3

The analysis of the system for a very particular condition $\alpha_k \rightarrow 0$ is used to demonstrate that the proposed strategy of control is global in this case, i.e. all controls are viable whatever the initial and final states. Let us make the following assumptions: it is possible to use ideal impulses (i.e. the velocity of m_2 can be changed instantaneously without modifying its position); it is possible to make t_i as small as desired; all the physical parameters of the system are known and the states are measurable. In order to simplify the notation, we define the initial conditions as

$$\{x_1(t_k) = x_1^{**}, \quad x_2(t_k) = x_2^{**}, \quad y_1(t_k^+) = y_1^{**}, \quad y_2(t_k^+) = y_2^{**}\}. \quad (66)$$

Given that we have supposed that the first impact occurs in the first constraint, the next physical conditions have to be satisfied:

$$x_1^{**} - x_2^{**} = L, \quad y_1^{**} - y_2^{**} < 0. \quad (67)$$

In addition let us assure that $y_1^{**} < 0$. The second condition in equation (67) of non-penetration is expressed in terms of the relative velocity between the masses. The desired target state is given by

$$\{x_1(t_{k+2}) = x_1^*, \quad x_2(t_{k+2}) = x_2^*, \quad y_1(t_{k+2}^+) = y_1^*, \quad y_2(t_{k+2}^+) = y_2^*\} \quad (68)$$

with

$$x_1^* - x_2^* = L, \quad y_1^* - y_2^* < 0 \quad (69)$$

For the first step, the target is determined by the conditions

$$\{x_1(t_{k+1}) = x_1^+, \quad x_2(t_{k+1}) = x_2^+, \quad y_1(t_{k+1}^+) = y_1^+ = -y_1^*, \quad y_2(t_{k+1}^+) = y_2^+\} \quad (70)$$

with

$$x_1^+ - x_2^+ = -L, \quad y_1^+ - y_2^+ > 0 \quad (71)$$

For this particular case, the dynamic equations describing the system between two consecutive collisions are given by

$$\begin{aligned}
 x_1(t_{k+1}) &= x_1(t_k) + y_1(t_k^+) \Delta_k \\
 y_1(t_{k+1}^-) &= y_1(t_k^+) \\
 x_2(t_{k+1}) &= x_2(t_k) + y_2(t_k^+) \Delta_k + \frac{\Lambda_k}{2} \Delta_k^2 \\
 y_2(t_{k+1}^-) &= y_2(t_k^+) + \Lambda_k \Delta_k
 \end{aligned} \tag{72}$$

It is important to note that the equation describing the system evolution depends only on the constant control between impacts. For the first phase in the limit when $\alpha_k \rightarrow 0$, the control inputs from equation (48) are given by

$$\begin{aligned}
 \lim_{\alpha_k \rightarrow 0} \Lambda_k &= \frac{2(x_2^+ - x_2^{**} - y_2^{**} \Delta_k^*)}{(\Delta_k^*)^2} \\
 \lim_{\alpha_k \rightarrow 0} p_k &= \frac{\Delta_k^* (y_1^+ - m_{11} y_1^{**} - m_{12} y_2^{**}) - 2m_{12} (x_2^+ - x_2^{**} - y_2^{**} \Delta_k^*)}{m_{12} \Delta_k^*} \\
 \Delta_k^* &= \frac{x_1^+ - x_1^{**}}{y_1^{**}}.
 \end{aligned} \tag{73}$$

We remark that p_k has a finite limit, hence there will be no penetration. The necessary condition to have the impact in the desired constraint is given by the inequality (see Appendix 5, equations (62)–(65)):

$$\Lambda_k = \frac{2(x_2^+ - x_2^{**} - y_2^{**} \Delta_k^*)}{(\Delta_k^*)^2} \geq -\frac{(y_1^{**} - y_2^{**})^2}{4L}. \tag{74}$$

Introducing equation (74) into the expression for Δ_k equal to that in equation (62) we can obtain

$$\Delta_k^* \leq \frac{-4L}{(y_1^{**} - y_2^{**})}. \tag{75}$$

Proceeding similarly for (t_{k+1}, t_{k+2}) from equation (50) we obtain

$$\begin{aligned}
 \lim_{\alpha_k \rightarrow 0} \Lambda_{k+1} &= \frac{2(x_2^* - x_2^+ - y_2^+ \Delta_{k+1}^*)}{(\Delta_{k+1}^*)^2} \\
 \lim_{\alpha_k \rightarrow 0} p_{k+1} &= \frac{\Delta_{k+1}^* (y_2^* - m_{21} y_1^+ - m_{22} y_2^+) - 2m_{22} (x_2^* - x_2^+ - y_2^+ \Delta_{k+1}^*)}{m_{22} \Delta_{k+1}^*} \\
 \Delta_{k+1}^* &= \frac{x_1^* - x_1^+}{y_1^+}
 \end{aligned} \tag{76}$$

and similarly to equations (74) and (75)

$$\Lambda_{k+1} = \frac{2(x_2^* - x_2^+ - y_2^+ \Delta_{k+1}^*)}{(\Delta_{k+1}^*)^2} \leq \frac{(y_1^+ - y_2^+)^2}{4L} \quad (77)$$

$$\Delta_{k+1}^* \leq \frac{4L}{(y_1^+ - y_2^+)}. \quad (78)$$

The condition in equation (74) can be expressed in terms of x_1^+ as

$$\frac{x_1^+ - x_1^{**}}{y_1^{**}} \geq \frac{-4L}{(y_1^{**} - y_2^{**})} \quad (79)$$

i.e.

$$\begin{aligned} x_1^+ &\leq x_1^{**} - \frac{4Ly_1^{**}}{y_1^{**} - y_2^{**}} \quad \text{if } y_1^{**} > 0 \\ x_1^+ &\geq x_1^{**} - \frac{4Ly_1^{**}}{y_1^{**} - y_2^{**}} \quad \text{if } y_1^{**} < 0. \end{aligned} \quad (80)$$

Similarly, equation (78) can be expressed as

$$\frac{x_1^* - x_1^+}{y_1^+} \leq \frac{4L}{(y_1^+ - y_2^+)}. \quad (81)$$

The velocities in the intermediate state are given by

$$\begin{aligned} y_1^+ &= -y_1^* \\ y_2^+ &= -\frac{m_{22}}{m_{12}}y_1^* + \left(m_{21} - \frac{m_{11}m_{22}}{m_{12}}\right)y_1^{**} \end{aligned} \quad (82)$$

so that, introducing equations (82) and (82) into equation (81), we obtain

$$x_1^+ \leq x_1^* + \frac{4Ly_1^*}{\psi(y_1^* + y_1^{**})} \quad (83)$$

where $\psi = \frac{e(1+\mu)}{1+e}$. Then, if we want to have a solution for $y_1^{**} < 0$, the conditions in equations (80) and (83) must be simultaneously satisfied. This is verified through the following expression:

$$x_1^+ \geq \max\left(x_1^{**} - \frac{4Ly_1^{**}}{y_1^{**} - y_2^{**}}, x_1^* + \frac{4Ly_1^*}{\psi(y_1^* + y_1^{**})}\right). \quad (84)$$

Remark 6. If $\alpha_k = 0$, then the closed-loop system is not well posed, because applying an impulsive input at an impact time requires much care (Brogliato, 1999). Therefore, this analysis should be limited to $\alpha_k \rightarrow 0$, and only points out how the control viability can be analyzed in a particular case.

APPENDIX C. STABILITY CONDITIONS

The characteristic polynomial can be divided as

$$h_3 Z^3 + h_2 Z^2 + h_1 Z + h_0 = (j_3 \zeta^3 + j_2 \zeta^2 + j_1 \zeta + j_0) (j_3 \zeta^3 - j_2 \zeta^2 + j_1 \zeta - j_0) \quad (85)$$

where $Z = \zeta^2$ and the coefficients j_3, j_2, j_1 and j_0 are given by

$$\begin{aligned} j_3 &= 3 \\ j_2 &= 2G(2 - G + e) - 3 \\ j_1 &= 2G(1 - G + 2e) - 3e^2 \\ j_0 &= 3e^2. \end{aligned} \quad (86)$$

It is easy to see that $|Z| < 1$ implies $|\zeta| < 1$. Thus, we can apply the Jury criterion to the equation $j_3 \zeta^3 + j_2 \zeta^2 + j_1 \zeta + j_0$ in order to obtain the conditions for stability. After some calculations, we have the following stability conditions

$$J_c^0 = 3 > 0 \quad (87)$$

$$J_c^1 = 3(1 - e^4) > 0 \quad (88)$$

$$J_c^2 = J_c^{2+} J_c^{2-} > 0 \quad (89)$$

$$J_c^3 = J_c^{3+} J_c^{3-} > 0 \quad (90)$$

where

$$\begin{aligned} J_c^{2+} &= 3(1 + e + e^2 + e^3) + 2(2e + e^2)G + 2(1 + e)(1 - G)G \\ J_c^{2-} &= 2G^2 + e^2 + 3e^3 + 2e(1 - G)^2 + (2 + e + 2e^2)(1 - G) + (1 - eG) \\ J_c^{3+} &= (1 - G)[4(1 + 3e + 2e^2 + 3e^3) + 10e^2(1 - G) + G^2 + 3(1 + 2e)(1 - G)^2] \\ &\quad + G(1 + 2eG^2 + 6eG) + 3e^3(2 + 3e) + 2(1 - e^2G) \\ J_c^{3-} &= 9e^3(1 + e) + G^2((2e^2 + 3e)(1 + G) + 2) + e(1 - eG) + 4(1 - e^2G) \\ &\quad (1 - G)[(2 + 5e + 2e^2)(1 - G)^2 + 3(1 + 4e + 5e^2 + 3e^3) + e^2]. \end{aligned} \quad (91)$$

From the above equations, we observe that if the viability condition in equation (19) is satisfied (which implies $0 < G \leq 1$) and $0 < e < 1$ then the conditions in equations (87)–(90) are always verified.

NOTES

1. In the following, we suppose that e is constant. However, we could use a more complex expression without calling into question the proposed analysis validity. Also $f(t^+) = \lim_{\tau \rightarrow t, \tau > t} f(\tau)$ and $f(t^-) = \lim_{\tau \rightarrow t, \tau < t} f(\tau)$.
2. The calculations are given in Appendix 5.

Acknowledgment. M. T. Mata-Jiménez is supported by CONACyT Mexico.

REFERENCES

- Abadie, M., 2000, "Dynamic simulation of rigid bodies: modelling of frictional contact," in *Impacts in Mechanical Systems. Analysis and Modelling, Lecture Notes in Physics*, 551, 61–144, B. Brogliato, ed., Springer, Berlin.
- Anglès, J., 1996, *Étude qualitative des vibrations en présence d'un obstacle d'un système mécanique*, PhD thesis, Université Paris XI Orsay.
- Azenha, A., and Tenreiro Machado, J. A., 1996, "Variable structure control of systems with nonlinear friction and dynamic backlash," in *Proceedings of the 13th World Congress of IFAC*, 515–520, July, San Francisco, USA.
- Babitsky, V. I., 1998, *Theory of Vibro-Impact Systems and Applications*. Foundation of Engineering Mechanics, Springer-Verlag.
- Bapat, C. N., Popplewell, N., and McLachlan, K., 1983, "Stable periodic motions of an impact-pair," *Journal of Sound and Vibration*, **87**(1), 19–40.
- Brogliato, B., 1999, *Nonsmooth Mechanics*, 2nd edition, CCES Springer-Verlag, London. Erratum and addendum at <http://www-lag.ensieg.inpg.fr/publications.html>
- Brogliato, B., 2001, "On the control of nonsmooth complementarity dynamical systems" in *Philosophical Transactions of the Royal Society, Special issue on Nonsmooth Mechanics*, **359**, 2369–2383.
- Brogliato, B., Niculescu, S., and Marques, M. M., 2000, "On tracking control of a class of complementary-slackness hybrid mechanical systems," *Systems and Control Letters*, **39**, 255–266.
- Brogliato, B., and Zavala Rio, A., 2000, "On the control of complementary-slackness juggling mechanical systems," *IEEE Transactions on Automatic Control*, **45**(2), 235–246.
- Chalhoub, N. G., and Zhang, X., 1996, "Modeling and control of backlash in the drive mechanism of a radially rotating compliant beam," *Journal of Dynamic Systems, Measurement, and Control*, **118**, 158–161.
- Choi, Y. S., and Noa, S. T., 1989, "Periodic response of a link coupling with clearance," *Journal of Dynamic Systems, Measurement, and Control*, **111**, 253–259.
-  Dagalakis, N. G., and Myers, D. R., 1985, "Adjustment of robot joint gears using encoder velocity and position information," *Journal of Robotic Systems*, **2**(2).
- Deck, J. F., and Dubowsky, S., 1994, "On the limitations of predictions of the dynamic response of machines with clearance connections," *ASME Journal of Mechanical Design*, **116**, 833–841.
- Fanuc, 1994, *FANUC Digital Servo ROM 9031 Series* FANUC Ltd.
- Grebogi, C., Ott, E., and Yorke, J. A., 1994, "Metamorphoses of basin boundaries in nonlinear dynamical systems," *Physical Review Letters*, **56**(3), 1011–1014.
- Guckenheimer, J., 1995, "A robust hybrid stabilization strategy for equilibria," *IEEE Transactions on Automatic Control*, **2**(40), 321–326.
- Heiman, M. S., Sherman, P. J., and Bajaj, K., 1987, "On the dynamics and stability of an inclined impact pair," *Journal of Sound and Vibration*, **114**(3), 535–547.
- Hsiao, F. H., and Hwang, J. D., 1997, "Optimal controller for dithered systems with backlash or hysteresis," *Optimization theory and applications*, **94**(1), 87–113.
- Hubbard, J., and West, H., 1995, *Differential equations: a dynamical systems approach. Higher dimensional systems*, Number 18 in Texts in Applied Mathematics, Springer-Verlag.
- Hung, R., and Pan, H., 1996, "Modelling of sloshing modulated angular momentum fluctuations actuated by gravity gradient associated with spacecraft slew motion," *Applied Mathematical Modelling*, **20**, 399–409.
- Ibrahim, R. A., and Sayad, M. A., 1999, "Nonlinear interaction of structural systems involving liquid sloshing impact loading," in *IUTAM Symposium on Unilateral Multibody Contacts*, Munich, Germany, August 1998, 97–106, Kluwer.
- Indri, M., and Tomambè, A., 1997, "Application of a PD controller on two mating gears with elasticity and backlash," in *Conference on Decision and Control*, San Diego, USA, December.
- Kunert, A., and Pfeiffer, F., 1991, "Description of chaotic motion by an invariant probability density," *Nonlinear Dynamics*, (2), 291–304.
- Li, G. X., Rand, R. H., and Moon, F. C., 1990, "Bifurcations and chaos in a forced zero-stiffness impact oscillator," *Journal of Non-linear Mechanics*, **25**(4), 417–432.
- L'otstedt, P., 1982, "Mechanical systems of rigid bodies subject to unilateral constraints," *SIAM, Journal of Applied Mathematics*, **42**(2), 281–296.
- Masri, S. F., and Caughey, T. K., 1966, "On the stability of the impact damper," *ASME Journal of Applied Mechanics*, **33**, 586–592.

- Mata-Jiménez, M. T., 1998, *Commande de systèmes mécaniques avec du jeu dynamique* PhD thesis, Institut National Polytechnique de Grenoble.
- Mata-Jiménez, M. T., and Brogliato, B., 1999, "On the PD regulation of mechanical systems with dynamic backlash," in *European Control Conference*, Karlsruhe, Germany, CD-Rom paper F800.
- Mata-Jiménez, M. T., Brogliato, B., and Goswami, A., 1997, "Analysis of PD control of mechanical systems with dynamic backlash," in *Proceedings of the MV2 Symposium on Active Control in Mechanical Engineering*, Jezequel, L., ed., Lyon, France, 311–322, MV2, A.A. Balkema/Rotterdam, 2000.
- Nordin, M., 1993, *Uncertain systems with backlash: Modelling, identification and Synthesis*, PhD thesis, Royal Institute of Technology, Stockholm, Sweden.
- Nordin, M., Galic, J., and Gutman, P.-O., 1997, "New models for backlash and gear play," *International Journal of Adaptive Control and Signal Processing*, **11**(1), 9–63.
- Ott, E., Grebogi, C., and Yorke, J. A., 1990, "Controlling chaos," *Physical Review Letters*, **64**(11), 1196–1199.
- Peterka, F., and Vacik, J., 1992, "Transition to chaotic motion in mechanical systems with impacts," *Journal of Sound and Vibration*, **154**(1), 95–115.
- Pfeiffer, F., and Glocker, C., 1996, *Multibody Dynamics with Unilateral Contacts*, John Wiley and Sons, New York.
- Pfeiffer, F., and Kunert, A., 1990, "Rattling models from deterministic to stochastic processes," *Nonlinear Dynamics*, (1), 63–74.
- Pilipchuk, V., and Ibrahim, R., 1997, "The dynamics of a nonlinear system simulating liquid sloshing impact in moving containers," *Journal of Sound and Vibration*, **205**(5), 593–615.
- Podsedkowski, L., 1992, "Méthode de mesure des jeux mécaniques dans une chaîne cinématique, en particulier des robots," Technical report, Polytechnic University Lodz.
- Podsedkowski, L., 1997, "Une méthode de mesure des jeux mécaniques sur les articulations de robots," *RAIRO-APII-JESA Journal Européen des Systèmes Automatisés*, **31**(1), 45–56.
- Reithmeier, E., 1991, *Periodic solutions of nonlinear dynamical systems*, Number 1483 in Lectures Notes in Mathematics, Springer, Berlin.
- Schatzman, M., 1998, "Uniqueness and continuous dependence on data for one-dimensional impact problem," *Mathematical Computing Modelling*, **28**(4–8), 1–18.
- Shaw, S. W., and Rand, R. H., 1989, "The transition to chaos in a simple mechanical system," *Journal of Non-linear Mechanics*, **24**(1), 41–56.
- Smith, D., 1983, *Gears and Vibrations A Basic Approach to Understanding Gear Noise*, McMillan Press.
- Stepanenko, Y., and Sankar, T. S., 1986, "Vibro-impact analysis of control systems with mechanical clearance and its application to robotic actuators," *Journal of Dynamic Systems, Measurement, and Control*, **108**, 9–16.
- Tang, Y. S., Kao, J. Y., and Lin, Y. S., 1997, "Identification of and compensation for backlash on the contouring accuracy of CNC machining centres," *International Journal of Advanced Manufacturing Technology*, **13**(2), 77–85.
- Tao, G., and Kokotovic, P. V., 1995, "Continuous-time adaptive control of systems with unknown backlash," *IEEE Transactions on Automatic Control*, **40**(6), 1083–1087.
- Tao, G., Ma, X., and Ling, 2001, "Optimal and nonlinear decoupling control of systems with sandwiched backlash," *Automatica*, **37**(2), 165–176.
- Vidyasagar, M., 1993, *Nonlinear Systems Analysis*, Prentice Hall, 2nd edition.
- Yeh, C. S., Fu, L. C., and Yang, J. H., 1996, "Nonlinear adaptive control of a two-axis gun turret system with backlash," in *Proceedings of the 13th Triennial World Congress IFAC*, San Francisco, USA, June 30–July 5.
- Zavala Río, A., and Brogliato, B., 1999, "On the control of a one degree-of freedom juggling robot," *Dynamics and Control*, **9**(1).

